Journal of Computational Physics 327 (2016) 270–293

Contents lists available at ScienceDirect

Journal of Computational Physics

www.elsevier.com/locate/jcp

A uniformly accurate multiscale time integrator spectral method for the Klein–Gordon–Zakharov system in the high-plasma-frequency limit regime

Weizhu Bao, Xiaofei Zhao *

Department of Mathematics, National University of Singapore, Singapore 119076, Singapore

ARTICLE INFO

Article history:
Received 10 June 2015
Received in revised form 18 September 2016
Accepted 19 September 2016
Available online 23 September 2016

Keywords:
Klein–Gordon–Zakharov system
High-plasma-frequency limit
Multiscale decomposition
Multiscale time integrator
Uniformly accurate
Spectral method
Limiting model
Bright soliton
Blow-up

ABSTRACT

A multiscale time integrator sine pseudospectral (MTI-SP) method is presented for discretizing the Klein–Gordon–Zakharov (KGZ) system with a dimensionless parameter $0 < \varepsilon \leq 1$, which is inversely proportional to the plasma frequency. In the high-plasma-frequency limit regime, i.e. $0 < \varepsilon \ll 1$, the solution of the KGZ system propagates waves with amplitude at $O(1)$ and wavelength at $O(\varepsilon^2)$ in time and $O(1)$ in space, which causes significantly numerical burdens due to the high oscillation in time. The main idea of the numerical method is to carry out a multiscale decomposition by frequency (MDF) to the electric field component of the solution at each time step and then apply the sine pseudospectral discretization for spatial derivatives followed by using the exponential wave integrator in phase space for integrating the MDF and the equation of the ion density component. The method is explicit and easy to be implemented. Extensive numerical results show that the MTI-SP method converges uniformly and optimally in space with exponential convergence rate if the solution is smooth, and uniformly in time with linear convergence rate at $O(\tau)$ for $\varepsilon \in (0, 1]$ with τ time step size and optimally with quadratic convergence rate at $O(\tau^2)$ in the regime when either $\varepsilon = O(1)$ or $0 < \varepsilon \leq \tau$. Thus the meshing strategy requirement (or ε-scalability) of the MTI-SP for the KGZ system in the high-plasma-frequency limit regime is $\tau = O(1)$ and $h = O(1)$ for $0 < \varepsilon \ll 1$, which is significantly better than classical methods in the literatures. Finally, we apply the MTI-SP method to study the convergence rates of the KGZ system to its limiting models in the high-plasma-frequency limit and the interactions of bright solitons of the KGZ system, and to identify certain parameter regimes that the solution of the KGZ system will be blow-up in one dimension.

© 2016 Elsevier Inc. All rights reserved.

1. Introduction

Consider the Klein–Gordon–Zakharov (KGZ) system in d dimensions ($d = 3, 2, 1$) [5,10,26,37]

$$\partial_{tt}\psi(\mathbf{x}, t) - 3v_0^2\Delta\psi(\mathbf{x}, t) + \omega_p^2\psi(\mathbf{x}, t) + \omega_p^2\phi(\mathbf{x}, t)\psi(\mathbf{x}, t) = 0, \tag{1.1a}$$

* Corresponding author.
E-mail addresses: matbaowz@nus.edu.sg (W. Bao), zhxfnus@gmail.com (X. Zhao).
URL: http://www.math.nus.edu.sg/~bao/ (W. Bao).

http://dx.doi.org/10.1016/j.jcp.2016.09.046
0021-9991/© 2016 Elsevier Inc. All rights reserved.

$$\partial_{tt}\phi(\mathbf{x},t) - c_s^2\Delta\phi(\mathbf{x},t) - \frac{n_0\varepsilon_0}{4mN_0}\Delta\left(\psi^2(\mathbf{x},t)\right) = 0, \qquad \mathbf{x}\in\mathbb{R}^d, \tag{1.1b}$$

where t is time, $\mathbf{x}\in\mathbb{R}^d$ is the spatial coordinate, $\psi := \psi(\mathbf{x},t)$ and $\phi := \phi(\mathbf{x},t)$ are real-valued functions representing the fast time scale component of the electric field raised by electrons and the derivation of ion density from its equilibrium, respectively. Here ω_p is the electron plasma frequency, c_s is the speed of sound, v_0 is the electron thermal velocity, n_0 is plasma charge number, ε_0 is vacuum dielectric constant, N_0 is electron density and m is ion mass. The KGZ system (1.1) is a classical model for describing the mutual interaction between the Langmuir waves and ion acoustic waves in a plasma [11,14] and is also adopted to model the strong Langmuir turbulence [29]. In fact, it can be derived from the two-fluid Euler–Maxwell system for the electrons, ions and electric field, by neglecting the magnetic field and further assuming that ions move much slower than electrons [10,33].

In order to scale the KGZ system (1.1), we introduce

$$\tilde{t} = \frac{t}{t_s}, \qquad \tilde{\mathbf{x}} = \frac{\mathbf{x}}{x_s}, \qquad \tilde{\psi}(\tilde{\mathbf{x}},\tilde{t}) = \frac{\psi(\mathbf{x},t)}{\psi_s}, \qquad \tilde{\phi}(\tilde{\mathbf{x}},\tilde{t}) = \frac{\phi(\mathbf{x},t)}{\phi_s}, \tag{1.2}$$

where x_s, t_s, ψ_s and ϕ_s are the dimensionless length unit, time unit, electric filed unit and ion density unit, respectively, satisfying $t_s = \frac{\omega_p x_s^2}{3v_0^2}$, $\phi_s = \frac{3v_0^2}{x_s^2\omega_p^2}$ and $\psi_s = \frac{v_0}{\omega_p}\sqrt{\frac{12mN_0}{n_0\varepsilon_0}}$. As pointed out in [10], in many physical situations where the thermal electron velocity is much larger than the ion-acoustic speed, i.e. $3v_0^2 \gg c_s^2$, it is worthwhile to consider the regime $\frac{3v_0^2}{x_s\omega_p c_s} \approx 1$ when the plasma frequency ω_p is large. Then by plugging (1.2) into (1.1), after a simple computation and removing all $\tilde{}$, we consider in this paper the following dimensionless KGZ system in d dimensions as

$$\varepsilon^2\partial_{tt}\psi(\mathbf{x},t) - \Delta\psi(\mathbf{x},t) + \frac{1}{\varepsilon^2}\psi(\mathbf{x},t) + \phi(\mathbf{x},t)\psi(\mathbf{x},t) = 0, \tag{1.3a}$$

$$\partial_{tt}\phi(\mathbf{x},t) - \Delta\phi(\mathbf{x},t) - \Delta\left(\psi^2(\mathbf{x},t)\right) = 0, \qquad \mathbf{x}\in\mathbb{R}^d, \tag{1.3b}$$

where ε is a dimensionless parameter inversely proportional to the plasma frequency and is given by

$$0 < \varepsilon := \frac{\sqrt{3}v_0}{x_s\omega_p} = \frac{\omega_s}{\omega_p} \le 1, \qquad \text{with} \quad \omega_s := \frac{\sqrt{3}v_0}{x_s}. \tag{1.4}$$

We remark here that if one chooses the dimensionless length unit $x_s = \frac{\sqrt{3}v_0}{\omega_p}$ and thus $t_s = \frac{\omega_p x_s^2}{3v_0^2} = \frac{1}{\omega_p}$, $\phi_s = \frac{3v_0^2}{x_s^2\omega_p^2} = 1$ and $\psi_s = \frac{v_0}{\omega_p}\sqrt{\frac{12mN_0}{n_0\varepsilon_0}}$ in (1.2), then $\varepsilon = 1$ in (1.4) and the KGZ system (1.3) with $\varepsilon = 1$ takes the form often appearing in the literature [11,14,25,26,35,36]. This choice of x_s is appropriate when the wave frequency is at the same order of the plasma frequency. However, when the wave frequency is much smaller than the plasma frequency, a different choice of x_s is more appropriate. Note that the choice of x_s determines the observation scale of the time evolution of the waves and decides: (i) which phenomena are 'visible' by asymptotic analysis, and (ii) which phenomena can be resolved in the numerical discretization by specified spatial/temporal grids. In fact, there are two important parameter regimes: One is when $\varepsilon = 1$ ($\Longleftrightarrow x_s = \frac{\sqrt{3}v_0}{\omega_p}$, $t_s = \frac{1}{\omega_p}$, $\phi_s = 1$ and $\psi_s = \frac{v_0}{\omega_p}\sqrt{\frac{12mN_0}{n_0\varepsilon_0}}$), then the KGZ system (1.3) describes the case that wave frequency is at the same order of the plasma frequency; the other one is when $0 < \varepsilon \ll 1$, then the KGZ system (1.3) is in the high-plasma-frequency limit regime.

To study the dynamics of the KGZ system (1.3), the initial data is usually given as

$$\psi(\mathbf{x},0) = \psi_0(\mathbf{x}), \quad \partial_t\psi(\mathbf{x},0) = \frac{1}{\varepsilon^2}\psi_1(\mathbf{x}), \quad \phi(\mathbf{x},0) = \phi_0(\mathbf{x}), \quad \partial_t\phi(\mathbf{x},0) = \phi_1(\mathbf{x}), \qquad \mathbf{x}\in\mathbb{R}^d, \tag{1.5}$$

where ψ_0, ψ_1, ϕ_0 and ϕ_1 are given real-valued functions which are independent of ε. The KGZ system (1.3) is time symmetric and it conserves the total *energy* [26,27]

$$\begin{aligned} E(t) &:= \int_{\mathbb{R}^d}\left[\varepsilon^2\left(\partial_t\psi\right)^2 + |\nabla\psi|^2 + \frac{1}{\varepsilon^2}\psi^2 + \frac{1}{2}|\nabla\varphi|^2 + \frac{1}{2}\phi^2 + \phi\psi^2\right]d\mathbf{x} \\ &= \int_{\mathbb{R}^d}\left[\frac{1}{\varepsilon^2}\psi_1^2 + |\nabla\psi_0|^2 + \frac{1}{\varepsilon^2}\psi_0^2 + \frac{1}{2}|\nabla\varphi_0|^2 + \frac{1}{2}\phi_0^2 + \phi_0\psi_0^2\right]d\mathbf{x} \equiv E(0), \qquad t \ge 0, \end{aligned} \tag{1.6}$$

where $\varphi(\mathbf{x},t)$ is defined via $\Delta\varphi(\mathbf{x},t) = \partial_t\phi(\mathbf{x},t)$ with $\lim_{|\mathbf{x}|\to\infty}\varphi(\mathbf{x},t) = 0$ for $t \ge 0$ and $\varphi_0(\mathbf{x}) = \Delta^{-1}\phi_1(\mathbf{x})$.

For the KGZ system (1.3) with $\varepsilon = 1$, i.e. O(1)-plasma-frequency regime, there are extensive analytical and numerical results in the literatures. For the existence and uniqueness as well as local ill-posedness in the energy space due to the lack of null form structure, we refer to [25,26] and references therein. For the numerical methods and comparison such as

the finite difference time domain (FDTD) methods and exponential-wave-integrator spectral method, we refer to [35,36,5,38] and references therein. However, for the KGZ system (1.3) with $0 < \varepsilon \ll 1$, i.e. high-plasma-frequency limit regime, the analysis and efficient computation of the KGZ system (1.3) are mathematically and numerically rather complicated issues [10,26]. The main difficulty is due to that the solution is highly oscillatory in time and the corresponding energy functional $E(t) = O(\varepsilon^{-2})$ in (1.6) becomes unbounded when $\varepsilon \to 0$.

Formally, in the high-plasma-frequency limit regime, i.e. $0 < \varepsilon \ll 1$, similar to the analysis of the nonrelativistic limit of the Klein–Gordon (KG) equation [28] and the Klein–Gordon-Schrödinger (KGS) equations [9], taking the ansatz

$$\psi(\mathbf{x}, t) = \mathrm{e}^{it/\varepsilon^2} z(\mathbf{x}, t) + \mathrm{e}^{-it/\varepsilon^2} \overline{z}(\mathbf{x}, t) + o(\varepsilon), \qquad \mathbf{x} \in \mathbb{R}^d, \quad t \geq 0, \tag{1.7}$$

where $\overline{z}$ denotes the complex conjugate of a complex-valued function z, and plugging it into (1.3) with (1.5), we can obtain — *a semi-limiting model* — the Zakharov system with wave operator

$$2i\partial_t z(\mathbf{x}, t) + \varepsilon^2 \partial_{tt} z(\mathbf{x}, t) - \Delta z(\mathbf{x}, t) + \phi(\mathbf{x}, t) z(\mathbf{x}, t) = 0, \tag{1.8a}$$

$$\partial_{tt} \phi(\mathbf{x}, t) - \Delta \phi(\mathbf{x}, t) - 2\Delta \left(|z(x, t)|^2 \right) = 0, \qquad \mathbf{x} \in \mathbb{R}^d, \quad t > 0, \tag{1.8b}$$

with the well-prepared (i.e. $\partial_t z(\mathbf{x}, 0)$ is obtained from (1.8a) by setting $t = 0$ and $\varepsilon = 0$ such that the leading oscillating term in the solution of (1.8) is due to the term $\varepsilon^2 \partial_{tt} z(\mathbf{x}, t)$ instead of the initial data) initial data [1,2]:

$$\begin{cases} z(\mathbf{x}, 0) = \dfrac{1}{2} \left[\psi_0(\mathbf{x}) - i\psi_1(\mathbf{x}) \right], \quad \partial_t z(\mathbf{x}, 0) = \dfrac{i}{2} \left[-\Delta z(\mathbf{x}, 0) + \phi_0(\mathbf{x}) z(\mathbf{x}, 0) \right], \\ \phi(\mathbf{x}, 0) = \phi_0(\mathbf{x}), \quad \partial_t \phi(\mathbf{x}, 0) = \phi_1(\mathbf{x}), \qquad \mathbf{x} \in \mathbb{R}^d. \end{cases} \tag{1.9}$$

In addition, after dropping the second term in (1.8a), we can get — *the limiting model* — the Zakharov system [10]

$$2i\partial_t z(\mathbf{x}, t) - \Delta z(\mathbf{x}, t) + \phi(\mathbf{x}, t) z(\mathbf{x}, t) = 0, \tag{1.10a}$$

$$\partial_{tt} \phi(\mathbf{x}, t) - \Delta \phi(\mathbf{x}, t) - 2\Delta \left(|z(\mathbf{x}, t)|^2 \right) = 0, \qquad \mathbf{x} \in \mathbb{R}^d, \quad t > 0, \tag{1.10b}$$

with the initial data

$$z(\mathbf{x}, 0) = \frac{1}{2} \left[\psi_0(\mathbf{x}) - i\psi_1(\mathbf{x}) \right], \quad \phi(\mathbf{x}, 0) = \phi_0(\mathbf{x}), \qquad \partial_t \phi(\mathbf{x}, 0) = \phi_1(\mathbf{x}), \qquad \mathbf{x} \in \mathbb{R}^d. \tag{1.11}$$

This formal analysis as well as recent analytical results [26,27] shows that the solution (ψ, ϕ) of the KGZ system (1.3) with (1.5) propagates waves with wavelength $O(\varepsilon^2)$ in time and $O(1)$ in space when $0 < \varepsilon \ll 1$. To illustrate the oscillation in this case, Fig. 1 shows the solutions $\psi(0, t)$, $\phi(0, t)$, $\psi(x, 2)$ and $\phi(x, 2)$ of the KGZ system (1.3) with (1.5) and $d = 1$, $\psi_0(x) = e^{-x^2/2}$, $\psi_1(x) = \frac{3}{2}\psi_0(x)$, $\phi_0(x) = \mathrm{sech}(x^2/2)$ and $\phi_1(x) = \mathrm{e}^{-x^2/2}$ for different ε.

This highly temporal oscillatory nature in the solution makes the numerical approximation of (1.3) extremely challenging and costly in the high-plasma-frequency limit regime, i.e. $0 < \varepsilon \ll 1$. Recently, different numerical methods have been proposed and analyzed as well as compared for the nonlinear KG equation and the KGS equations in the nonrelativistic limit regime in which the solutions share similar oscillatory behavior as that of the KGZ system (1.3), including the FDTD methods [4], exponential wave integrator Fourier pseudospectral (EWI-FP) method [4,5,9], asymptotic preserving (AP) method [16], stroboscopic average method (SAM) [12] and multiscale time integrator Fourier pseudospectral (MTI-FP) method [3], etc. Among them, the MTI-FP method is uniformly convergent (UA) for $\varepsilon \in (0, 1]$ and it is the most efficient from the practical computation point of view, while the FDTD, EWI-FP and AP methods are not UA methods. The main aim of this paper is to propose and analyze a multiscale time integrator sine pseudospectral (MTI-SP) method for the KGZ system (1.3) in the high-plasma-frequency limit regime by adapting a multiscale decomposition by frequency to the solution at each time step and applying the sine pseudospectral discretization and exponential wave integrators (EWIs) for spatial and temporal derivatives, respectively. We will study numerically spatial and temporal accuracy for fixed $0 < \varepsilon \leq 1$ and ε-scalability (or ε-resolution) when $0 < \varepsilon \ll 1$ of the proposed MTI-SP method, and compare its performance with existing numerical methods in the literature for the KGZ system. Then we apply the MTI-SP method to study numerically convergence rates of the KGZ system (1.3) to its limiting models including the Zakharov system with wave operator (1.8)–(1.9) and the Zakharov system (1.10)–(1.11). Finally, we apply it to simulate some very interesting dynamics of the KGZ system, including the stability and collision of bright solitons in one dimension (1D), parameter regimes where the solution blows up at finite time in 1D and the interaction of waves in two dimensions (2D).

The paper is organized as follows. In section 2, we present a multiscale decomposition by frequency (MDF) for the solution of the KGZ system. In section 3, we propose an MTI-SP method for discretizing the KGZ system based on the MDF. Numerical studies and results are given in section 4. Finally, some concluding remarks are drawn in section 5. Throughout the paper we denote $p \lesssim q$ to represent that there exists a generic constant $C > 0$ which is independent of τ, h and ε, such that $|p| \leq Cq$.

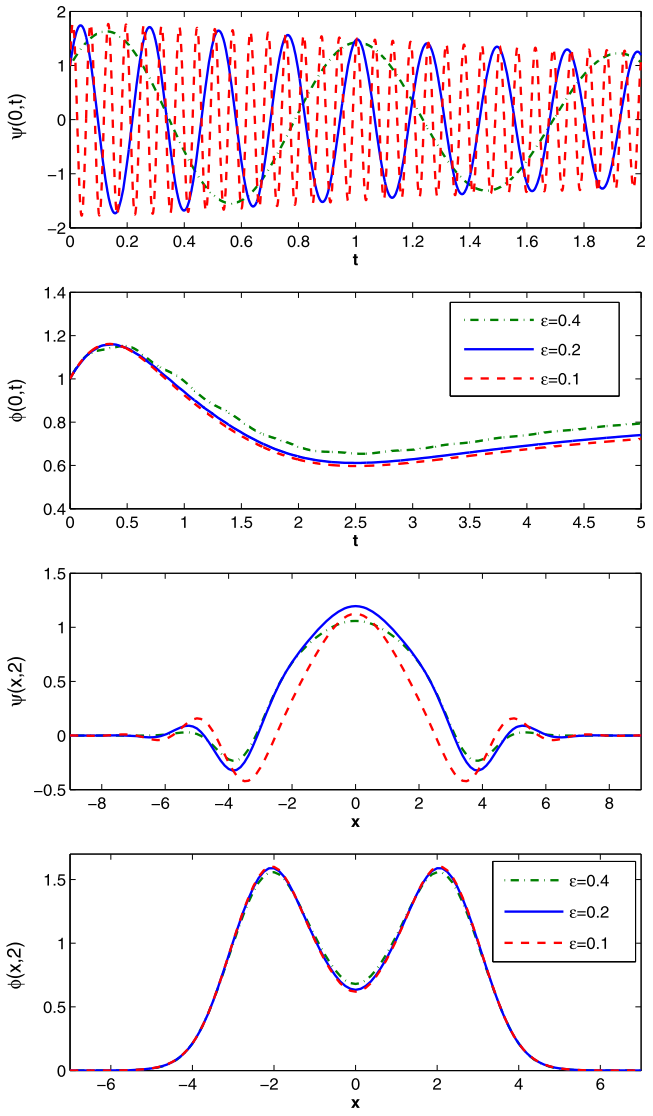

Fig. 1. Profile of the solution of the KGZ system (1.3) with (1.5) and $d = 1$ for different ε.

2. A multiscale decomposition

Let $\tau = \Delta t > 0$ be the time step size, and denote time steps by $t_n = n\tau$ for $n = 0, 1, \ldots$. In this section, we present a multiscale decomposition for the solution of the KGZ system (1.3) on the time interval $[t_n, t_{n+1}]$ with given initial data at $t = t_n$ as

$$\psi(\mathbf{x}, t_n) = \psi_0^n(\mathbf{x}) = O(1), \qquad \partial_t \psi(\mathbf{x}, t_n) = \frac{1}{\varepsilon^2}\psi_1^n(\mathbf{x}) = O\left(\frac{1}{\varepsilon^2}\right), \tag{2.1a}$$

$$\phi(\mathbf{x}, t_n) = \phi_0^n(\mathbf{x}) = O(1), \qquad \partial_t \phi(\mathbf{x}, t_n) = \phi_1^n(\mathbf{x}) = O(1), \qquad \mathbf{x} \in \mathbb{R}^d. \tag{2.1b}$$

Similar to the analysis of the nonrelativistic limits of the nonlinear KG equation [28,6,3] and the KGS equations [9], we take an ansatz as $\psi(\mathbf{x}, t) := \psi(\mathbf{x}, t_n + s)$ of (1.3a) on $[t_n, t_{n+1}]$ with (2.1) as

$$\psi(\mathbf{x}, t_n + s) = \mathrm{e}^{is/\varepsilon^2} z^n(\mathbf{x}, s) + \mathrm{e}^{-is/\varepsilon^2}\overline{z^n}(\mathbf{x}, s) + r^n(\mathbf{x}, s), \quad \mathbf{x} \in \mathbb{R}^d, \ \ 0 \le s \le \tau, \tag{2.2}$$

where $z^n(\mathbf{x}, s)$ is a complex-valued function and $r^n(\mathbf{x}, s)$ is a real-valued function, satisfying $z^n(\mathbf{x}, s) = O(1)$, $\partial_s z^n(\mathbf{x}, s) = O(1)$, $\partial_{ss} z^n(\mathbf{x}, s) = O(1)$, $r^n(\mathbf{x}, s) = O(\varepsilon^2)$, $\partial_s r^n(\mathbf{x}, s) = O(1)$ and $\partial_{ss} r^n(\mathbf{x}, s) = O(\varepsilon^{-2})$ for $\mathbf{x} \in \mathbb{R}^d$, $0 \le s \le \tau$ and $0 < \varepsilon \le 1$. Differentiating (2.2) with respect to s, we have for $\mathbf{x} \in \mathbb{R}^d$ and $0 \le s \le \tau$

$$\partial_s\psi(\mathbf{x},t_n+s)=\mathrm{e}^{is/\varepsilon^2}\left[\partial_s z^n(\mathbf{x},s)+\frac{i}{\varepsilon^2}z^n(\mathbf{x},s)\right]+\partial_s r^n(\mathbf{x},s)+\mathrm{e}^{-is/\varepsilon^2}\left[\partial_s\overline{z^n}(\mathbf{x},s)-\frac{i}{\varepsilon^2}\overline{z^n}(\mathbf{x},s)\right]. \tag{2.3}$$

Plugging (2.2) into (1.3a), we get for $\mathbf{x}\in\mathbb{R}^d$, $0\le s\le\tau$ and $\phi(\mathbf{x},t_n+s)=:\phi^n(\mathbf{x},s)$

$$\begin{aligned}&\mathrm{e}^{is/\varepsilon^2}\Big[\varepsilon^2\partial_{ss}z^n(\mathbf{x},s)+2i\partial_s z^n(\mathbf{x},s)-\Delta z^n(\mathbf{x},s)+z^n(\mathbf{x},s)\phi^n(\mathbf{x},s)\Big]+\mathrm{e}^{-is/\varepsilon^2}\Big[\varepsilon^2\partial_{ss}\overline{z^n}(\mathbf{x},s)-\Delta\overline{z^n}(\mathbf{x},s)\\&\quad-2i\partial_s\overline{z^n}(\mathbf{x},s)+\overline{z^n}(\mathbf{x},s)\phi^n(\mathbf{x},s)\Big]+\varepsilon^2\partial_{ss}r^n(\mathbf{x},s)-\Delta r^n(\mathbf{x},s)+\frac{1}{\varepsilon^2}r^n(\mathbf{x},s)+r^n(\mathbf{x},s)\phi^n(\mathbf{x},s)=0.\end{aligned}$$

Multiplying the above equation by $\mathrm{e}^{-is/\varepsilon^2}$ and $\mathrm{e}^{is/\varepsilon^2}$, respectively, we can decompose it into a coupled system for two ε^2-frequency waves with the unknown $z^n(\mathbf{x},s):=z^n$ and the rest frequency waves with the unknown $r^n(\mathbf{x},s):=r^n$ as

$$\begin{cases}2i\partial_s z^n+\varepsilon^2\partial_{ss}z^n-\Delta z^n+z^n\phi^n=0,\\ \varepsilon^2\partial_{ss}r^n-\Delta r^n+\dfrac{1}{\varepsilon^2}r^n+r^n\phi^n=0,\end{cases}\qquad \mathbf{x}\in\mathbb{R}^d,\quad 0\le s\le\tau. \tag{2.4}$$

Substituting (2.2) into (1.3b), we get

$$\begin{cases}\partial_{ss}\phi^n-\Delta\phi^n-\mathrm{e}^{2is/\varepsilon^2}\Delta\left((z^n)^2\right)-\mathrm{e}^{-2is/\varepsilon^2}\Delta\left((\overline{z^n})^2\right)-2\mathrm{e}^{is/\varepsilon^2}\Delta\left(z^n r^n\right)\\ \qquad-2\mathrm{e}^{-is/\varepsilon^2}\Delta\left(\overline{z^n}r^n\right)-\Delta\left(2|z^n|^2+|r^n|^2\right)=0,\qquad \mathbf{x}\in\mathbb{R}^d,\ \ 0<s\le\tau,\\ \phi^n(\mathbf{x},0)=\phi_0^n(\mathbf{x}),\quad \partial_s\phi^n(\mathbf{x},0)=\phi_1^n(\mathbf{x}),\qquad \mathbf{x}\in\mathbb{R}^d.\end{cases} \tag{2.5}$$

In order to find proper initial conditions for the system (2.4) coupled with (2.5), setting $s=0$ in (2.2) and (2.3), noticing (2.1a), we obtain

$$\begin{cases}z^n(\mathbf{x},0)+\overline{z^n}(\mathbf{x},0)+r^n(\mathbf{x},0)=\psi_0^n(\mathbf{x}),\qquad \mathbf{x}\in\mathbb{R}^d,\\ \dfrac{i}{\varepsilon^2}\left[z^n(\mathbf{x},0)-\overline{z^n}(\mathbf{x},0)\right]+\partial_s z^n(\mathbf{x},0)+\partial_s\overline{z^n}(\mathbf{x},0)+\partial_s r^n(\mathbf{x},0)=\dfrac{1}{\varepsilon^2}\psi_1^n(\mathbf{x}).\end{cases} \tag{2.6}$$

Now we decompose the above initial data so as to: (i) equate $O\left(\frac{1}{\varepsilon^2}\right)$ and $O(1)$ terms in the second equation of (2.6), respectively, and (ii) be well-prepared for the first equation in (2.4) when $0<\varepsilon\ll 1$, i.e. $\partial_s z^n(\mathbf{x},0)$ is determined from the first equation in (2.4) by setting $\varepsilon=0$ and $s=0$ [1–3]:

$$\begin{cases}z^n(\mathbf{x},0)+\overline{z^n}(\mathbf{x},0)=\psi_0^n(\mathbf{x}),\qquad i\left[z^n(\mathbf{x},0)-\overline{z^n}(\mathbf{x},0)\right]=\psi_1^n(\mathbf{x}),\qquad r^n(\mathbf{x},0)=0,\qquad \mathbf{x}\in\mathbb{R}^d,\\ 2i\partial_s z^n(\mathbf{x},0)-\Delta z^n(\mathbf{x},0)+z^n(\mathbf{x},0)\phi^n(\mathbf{x},0)=0,\qquad \partial_s r^n(\mathbf{x},0)+\partial_s z^n(\mathbf{x},0)+\partial_s\overline{z^n}(\mathbf{x},0)=0.\end{cases} \tag{2.7}$$

Solving (2.7), we get the initial data for (2.4) as

$$\begin{cases}z^n(\mathbf{x},0)=\dfrac{1}{2}\left[\psi_0^n(\mathbf{x})-i\psi_1^n(\mathbf{x})\right],\quad \partial_s z^n(\mathbf{x},0)=\dfrac{i}{2}\left[-\Delta z^n(\mathbf{x},0)+z^n(\mathbf{x},0)\phi_0^n(\mathbf{x})\right],\\ r^n(\mathbf{x},0)\equiv 0,\qquad \partial_s r^n(\mathbf{x},0)=-\partial_s z^n(\mathbf{x},0)-\partial_s\overline{z^n}(\mathbf{x},0),\qquad \mathbf{x}\in\mathbb{R}^d.\end{cases} \tag{2.8}$$

The above decomposition can be called as multiscale decomposition by frequency (MDF). In fact, it can also be regarded as to decompose slow waves at ε^2-wavelength and fast waves at other wavelengths, thus it can also be called as fast–slow frequency decomposition. After solving the decomposed system (2.4)–(2.5) with the initial data (2.8), we get $\phi^n(\mathbf{x},\tau)=:\phi_0^{n+1}(\mathbf{x})$, $\partial_s\phi^n(\mathbf{x},\tau)=:\phi_1^{n+1}(\mathbf{x})$, $z^n(\mathbf{x},\tau)$, $\partial_s z^n(\mathbf{x},\tau)$, $r^n(\mathbf{x},\tau)$ and $\partial_s r^n(\mathbf{x},\tau)$ for $\mathbf{x}\in\mathbb{R}^d$. Then we can reconstruct the solution ψ to (1.3a) at $t=t_{n+1}$ by setting $s=\tau$ in (2.2) and (2.3), i.e.,

$$\psi(\mathbf{x},t_{n+1})=\mathrm{e}^{i\tau/\varepsilon^2}z^n(\mathbf{x},\tau)+\mathrm{e}^{-i\tau/\varepsilon^2}\overline{z^n}(\mathbf{x},\tau)+r^n(\mathbf{x},\tau)=:\psi_0^{n+1}(\mathbf{x}),\quad \partial_t\psi(\mathbf{x},t_{n+1})=\frac{1}{\varepsilon^2}\psi_1^{n+1}(\mathbf{x}), \tag{2.9}$$

with

$$\psi_1^{n+1}(\mathbf{x}):=\mathrm{e}^{i\tau/\varepsilon^2}\left[\varepsilon^2\partial_s z^n(\mathbf{x},\tau)+iz^n(\mathbf{x},\tau)\right]+\mathrm{e}^{-i\tau/\varepsilon^2}\left[\varepsilon^2\partial_s\overline{z^n}(\mathbf{x},\tau)-i\overline{z^n}(\mathbf{x},\tau)\right]+\varepsilon^2\partial_s r^n(\mathbf{x},\tau),\quad \mathbf{x}\in\mathbb{R}^d.$$

In summary, the MDF proceeds as a decomposition–propagation–reconstruction flow at each time interval and thus it is different with the modulated Fourier expansion [13,23,32] which carries out the decomposition only at $t=0$.

Let $0<T<T^*$ with T^* the maximum existence time of the solution of the KGZ system (1.3) with (1.5) [26,27,30], we assume that its solution satisfies $\psi\in C^1\left([0,T];H^4\right)$, $\phi\in C^1\left([0,T];H^3\right)$ and

$$\|\psi\|_{L^\infty([0,T];H^4)}+\varepsilon^2\|\partial_t\psi\|_{L^\infty([0,T];H^4)}\lesssim 1,\qquad \|\phi\|_{L^\infty([0,T];H^3)}+\|\partial_t\phi\|_{L^\infty([0,T];H^3)}\lesssim 1.$$

Similar to the MDF decomposition of the nonlinear KG equation [3] and the KGS equations [9] with the detailed proof omitted here for brevity, we can show that there exists a constant $\tau_1 > 0$ independent of $0 < \varepsilon \leq 1$ such that for any $0 < \tau \leq \tau_1$

$$\begin{aligned}
&\left\|z^n\right\|_{L^\infty([0,\tau];H^2)} + \left\|\partial_s z^n\right\|_{L^\infty([0,\tau];H^1)} + \left\|\partial_{ss} z^n\right\|_{L^\infty([0,\tau];L^2)} \lesssim 1, \qquad 0 \leq n < \frac{T}{\tau},\\
&\left\|r^n\right\|_{L^\infty([0,\tau];H^2)} + \varepsilon^2 \left\|\partial_s r^n\right\|_{L^\infty([0,\tau];H^1)} + \varepsilon^4 \left\|\partial_{ss} r^n\right\|_{L^\infty([0,\tau];L^2)} \lesssim \varepsilon^2.
\end{aligned}$$

3. An MTI-SP method

For the simplicity of notations and without of loss generality, we shall only present the method in 1D. Generalizations to higher dimensions are straightforward and the results remain valid. We truncate the whole space problem (1.3) with (1.5) into a finite interval $\Omega = (a, b)$ with homogeneous Dirichlet boundary conditions, where due to the fast decay of the solution at far field, the truncation error can be negligible by choosing a, b sufficiently large. In 1D, the problem reduces to

$$\begin{cases}
\varepsilon^2 \partial_{tt}\psi(x,t) - \partial_{xx}\psi(x,t) + \dfrac{1}{\varepsilon^2}\psi(x,t) + \psi(x,t)\phi(x,t) = 0, \quad x \in \Omega,\ t > 0,\\
\partial_{tt}\phi(x,t) - \partial_{xx}\phi(x,t) - \partial_{xx}\left(\psi^2(x,t)\right) = 0, \quad x \in \Omega, \quad t > 0,\\
\psi(a,t) = \psi(b,t) = 0, \quad \phi(a,t) = \phi(b,t) = 0, \quad t \geq 0,\\
\psi(x,0) = \psi_0(x),\ \partial_t\psi(x,0) = \dfrac{1}{\varepsilon^2}\psi_1(x),\ \phi(x,0) = \phi_0(x),\ \partial_t\phi(x,0) = \phi_1(x), \quad x \in \overline{\Omega} = [a,b].
\end{cases} \tag{3.1}$$

We remark that the boundary conditions considered here are inspired by the inherent physical nature of the system and they have been widely used in the literature for the simulation of the dynamics of the KGZ system (see, e.g. [26,30,36,38] and references therein).

Consequently, for $n \geq 0$, the decomposed system MDF (2.4)–(2.5) in 1D reduces to

$$\begin{cases}
2i\partial_s z^n + \varepsilon^2\partial_{ss} z^n - \partial_{xx} z^n + z^n\phi^n = 0, \qquad \varepsilon^2\partial_{ss} r^n - \partial_{xx} r^n + \dfrac{1}{\varepsilon^2} r^n + r^n\phi^n = 0,\\
\partial_{ss}\phi^n - \partial_{xx}\phi^n - \mathrm{e}^{2is/\varepsilon^2}\partial_{xx}\left((z^n)^2\right) - \mathrm{e}^{-2is/\varepsilon^2}\partial_{xx}\left((\overline{z^n})^2\right) - 2\mathrm{e}^{is/\varepsilon^2}\partial_{xx}\left(z^n r^n\right)\\
\qquad - 2\mathrm{e}^{-is/\varepsilon^2}\partial_{xx}\left(\overline{z^n} r^n\right) - \partial_{xx}\left(2|z^n|^2 + |r^n|^2\right) = 0, \qquad a < x < b, \quad 0 < s \leq \tau.
\end{cases} \tag{3.2}$$

The initial and boundary conditions for the above system are

$$\begin{cases}
z^n(a,s) = z^n(b,s) = 0, \quad r^n(a,s) = r^n(b,s) = 0, \quad \phi^n(a,s) = \phi^n(b,s) = 0, \quad 0 \leq s \leq \tau;\\
z^n(x,0) = \dfrac{1}{2}\left[\psi_0^n(x) - i\psi_1^n(x)\right], \quad \partial_s z^n(x,0) = \dfrac{i}{2}\left[-\partial_{xx} z^n(x,0) + z^n(x,0)\phi_0^n(x)\right], \quad a \leq x \leq b,\\
r^n(x,0) \equiv 0, \quad \partial_s r^n(x,0) = -\partial_s z^n(x,0) - \partial_s\overline{z^n}(x,0), \quad \phi^n(x,0) = \phi_0^n(x), \quad \partial_s\phi^n(x,0) = \phi_1^n(x).
\end{cases} \tag{3.3}$$

We now present an exponential wave integrator (EWI) sine spectral/pseudospectral discretization for the MDF (3.2) with (3.3), which applies the sine spectral/pseudospectral discretization to spatial derivatives followed by using some proper EWIs [4,19,20,22,23] for temporal discretizations in phase space.

Choose the mesh size $h := \Delta x = (b-a)/N$ with N a positive integer and denote grid points as $x_j := a + jh$ for $j = 0, 1, \ldots, N$. Define

$$\begin{aligned}
&X_N := \mathrm{span}\left\{\sin(\mu_l(x-a)) \ :\ x \in \overline{\Omega},\ \mu_l = \frac{\pi l}{b-a},\ l = 1, \ldots, N-1\right\},\\
&Y_N := \left\{\mathbf{v} = (v_0, v_1, \ldots, v_N)^T \in \mathbb{C}^{N+1} \mid v_0 = v_N = 0\right\}, \quad \text{with } \|\mathbf{v}\|_{l^2} = h\sum_{j=1}^{N-1}|v_j|^2.
\end{aligned}$$

For a function $v(x) \in H_0^1(\Omega)$ and a vector $\mathbf{v} \in Y_N$, let $P_N : H_0^1(\Omega) \to X_N$ be the L^2-projection operator, and $I_N : C(\Omega) \cap H_0^1(\Omega) \to X_N$ or $Y_N \to X_N$ be the trigonometric interpolation operator [18,31], i.e.

$$(P_N v)(x) = \sum_{l=1}^{N-1}\widehat{v}_l \sin(\mu_l(x-a)), \quad (I_N\mathbf{v})(x) = \sum_{l=1}^{N-1}\widetilde{v}_l \sin(\mu_l(x-a)), \tag{3.4}$$

where $\widehat{v}_l$ and $\widetilde{v}_l$ are the sine and discrete sine transform coefficients of the function $v(x)$ and vector $\mathbf{v}$ (with $v_j = v(x_j)$ for $j = 0, 1, \ldots, N$ when they are involved), respectively, defined as

$$\widehat{v}_l = \frac{2}{b-a}\int_a^b v(x)\sin(\mu_l(x-a))dx, \qquad \widetilde{v}_l = \frac{2}{N}\sum_{j=1}^{N-1} v_j \sin(\mu_l(x_j-a)). \tag{3.5}$$

Then a sine spectral method for discretizing (3.2) reads:

Find $z_N^n := z_N^n(x,s)$, $r_N^n := r_N^n(x,s)$, $\phi_N^n := \phi_N^n(x,s) \in X_N$ for $0 \le s \le \tau$, i.e.

$$\begin{cases} z_N^n(x,s) = \displaystyle\sum_{l=1}^{N-1} \widehat{(z_N^n)}_l(s)\sin(\mu_l(x-a)), \quad r_N^n(x,s) = \sum_{l=1}^{N-1} \widehat{(r_N^n)}_l(s)\sin(\mu_l(x-a)), \\ \phi_N^n(x,s) = \displaystyle\sum_{l=1}^{N-1} \widehat{(\phi_N^n)}_l(s)\sin(\mu_l(x-a)), \qquad a \le x \le b, \end{cases} \tag{3.6}$$

such that

$$\begin{cases} \varepsilon^2\partial_{ss} z_N^n + 2i\partial_s z_N^n - \partial_{xx} z_N^n + P_N\left(z_N^n\phi_N^n\right) = 0, \qquad a < x < b, \qquad 0 < s < \tau, \\ \varepsilon^2\partial_{ss} r_N^n - \partial_{xx} r_N^n + \dfrac{1}{\varepsilon^2} r_N^n + P_N(r_N^n\phi_N^n) = 0, \qquad \partial_{ss}\phi_N^n - \partial_{xx}\phi_N^n - \partial_{xx} P_N f_N^n(x,s) = 0, \end{cases} \tag{3.7}$$

where

$$\begin{aligned} f_N^n(x,s) := {} & \mathrm{e}^{2is/\varepsilon^2}\left(z_N^n\right)^2 + \mathrm{e}^{-2is/\varepsilon^2}\left(\overline{z_N^n}\right)^2 + 2\mathrm{e}^{is/\varepsilon^2}\left(z_N^n r_N^n\right) + 2\mathrm{e}^{-is/\varepsilon^2}\left(\overline{z_N^n} r_N^n\right) \\ & + 2|z_N^n|^2 + (r_N^n)^2, \qquad a < x < b, \qquad 0 < s < \tau. \end{aligned} \tag{3.8}$$

Substituting (3.6) into (3.7) and noticing the orthogonality of $\{\sin(\mu_l(x-a))\}_{l=1}^{N-1}$, we get

$$\begin{cases} \varepsilon^2 \widehat{(z_N^n)}_l''(s) + 2i\widehat{(z_N^n)}_l'(s) + \mu_l^2\widehat{(z_N^n)}_l(s) + \widehat{(z_N^n\phi_N^n)}_l(s) = 0, \qquad 0 < s \le \tau, \qquad 1 \le l \le N-1, \\ \varepsilon^2 \widehat{(r_N^n)}_l''(s) + \left(\mu_l^2 + \dfrac{1}{\varepsilon^2}\right)\widehat{(r_N^n)}_l(s) + \widehat{(r_N^n\phi_N^n)}_l(s) = 0, \quad \widehat{(\phi_N^n)}_l''(s) + \mu_l^2\widehat{(\phi_N^n)}_l(s) + \mu_l^2\widehat{(f_N^n)}_l(s) = 0. \end{cases} \tag{3.9}$$

In order to apply the EWIs to integrate (3.9) in time, for each fixed $1 \le l \le N-1$, we rewrite (3.9) by using the variation-of-constant formulas

$$\begin{cases} \widehat{(z_N^n)}_l(s) = a_l(s)\widehat{(z_N^n)}_l(0) + \varepsilon^2 b_l(s)\widehat{(z_N^n)}_l'(0) - \displaystyle\int_0^s b_l(s-\theta)\widehat{(z_N^n\phi_N^n)}_l(\theta)\,d\theta, \\ \widehat{(r_N^n)}_l(s) = \dfrac{\sin(\omega_l s)}{\omega_l}\widehat{(r_N^n)}_l'(0) - \displaystyle\int_0^s \frac{\sin(\omega_l(s-\theta))}{\varepsilon^2\omega_l}\widehat{(r_N^n\phi_N^n)}_l(\theta)\,d\theta, \qquad 0 \le s \le \tau, \\ \widehat{(\phi_N^n)}_l(s) = \cos(\mu_l s)\widehat{(\phi_N^n)}_l(0) + \dfrac{\sin(\mu_l s)}{\mu_l}\widehat{(\phi_N^n)}_l'(0) - \mu_l\displaystyle\int_0^s \sin(\mu_l(s-\theta))\,\widehat{(f_N^n)}_l(\theta)\,d\theta, \end{cases} \tag{3.10}$$

where

$$\begin{cases} a_l(s) := \dfrac{\lambda_l^+\mathrm{e}^{is\lambda_l^-} - \lambda_l^-\mathrm{e}^{is\lambda_l^+}}{\lambda_l^+ - \lambda_l^-}, \qquad b_l(s) := i\dfrac{\mathrm{e}^{is\lambda_l^+} - \mathrm{e}^{is\lambda_l^-}}{\varepsilon^2(\lambda_l^- - \lambda_l^+)}, \qquad 0 \le s \le \tau, \\ \lambda_l^\pm = -\dfrac{1}{\varepsilon^2}\left(1 \pm \sqrt{1+\mu_l^2\varepsilon^2}\right), \qquad \omega_l = \dfrac{\sqrt{1+\mu_l^2\varepsilon^2}}{\varepsilon^2}. \end{cases} \tag{3.11}$$

Differentiating (3.10) with respect to s, we obtain

$$\begin{cases} \widehat{(z_N^n)_l}'(s) = a_l'(s)\widehat{(z_N^n)_l}(0) + \varepsilon^2 b_l'(s)\widehat{(z_N^n)_l}'(0) - \displaystyle\int_0^s b_l'(s-\theta)\widehat{(z_N^n\phi_N^n)_l}(\theta)\,d\theta, \\ \widehat{(r_N^n)_l}'(s) = \cos(\omega_l s)\widehat{(r_N^n)_l}'(0) - \displaystyle\int_0^s \frac{\cos\left(\omega_l(s-\theta)\right)}{\varepsilon^2}\widehat{(r_N^n\phi_N^n)_l}(\theta)\,d\theta, \qquad 0 \le s \le \tau, \\ \widehat{(\phi_N^n)_l}'(s) = -\mu_l \sin(\mu_l s)\widehat{(\phi_N^n)_l}(0) + \cos(\mu_l s)\widehat{(\phi_N^n)_l}'(0) - \mu_l^2 \displaystyle\int_0^s \cos\left(\mu_l(s-\theta)\right)\widehat{(f_N^n)_l}(\theta)\,d\theta, \end{cases} \tag{3.12}$$

where

$$a_l'(s) = i\lambda_l^+\lambda_l^- \frac{e^{is\lambda_l^-} - e^{is\lambda_l^+}}{\lambda_l^+ - \lambda_l^-}, \quad b_l'(s) = \frac{\lambda_l^+ e^{is\lambda_l^+} - \lambda_l^- e^{is\lambda_l^-}}{\varepsilon^2(\lambda_l^+ - \lambda_l^-)}, \quad 0 \le s \le \tau.$$

Taking $s = \tau$ in (3.10) and (3.12), and using (3.8), we get

$$\begin{cases} \widehat{(z_N^n)_l}(\tau) = a_l(\tau)\widehat{(z_N^n)_l}(0) + \varepsilon^2 b_l(\tau)\widehat{(z_N^n)_l}'(0) - \displaystyle\int_0^\tau b_l(\tau-\theta)\widehat{(z_N^n\phi_N^n)_l}(\theta)\,d\theta, \\ \widehat{(z_N^n)_l}'(\tau) = a_l'(\tau)\widehat{(z_N^n)_l}(0) + \varepsilon^2 b_l'(\tau)\widehat{(z_N^n)_l}'(0) - \displaystyle\int_0^\tau b_l'(\tau-\theta)\widehat{(z_N^n\phi_N^n)_l}(\theta)\,d\theta, \\ \widehat{(r_N^n)_l}(\tau) = \dfrac{\sin(\omega_l\tau)}{\omega_l}\widehat{(r_N^n)_l}'(0) - \displaystyle\int_0^\tau \frac{\sin\left(\omega_l(\tau-\theta)\right)}{\varepsilon^2\omega_l}\widehat{(r_N^n\phi_N^n)_l}(\theta)\,d\theta, \\ \widehat{(r_N^n)_l}'(\tau) = \cos(\omega_l\tau)\widehat{(r_N^n)_l}'(0) - \displaystyle\int_0^\tau \frac{\cos\left(\omega_l(\tau-\theta)\right)}{\varepsilon^2}\widehat{(r_N^n\phi_N^n)_l}(\theta)\,d\theta, \\ \widehat{(\phi_N^n)_l}(\tau) = \cos(\mu_l\tau)\widehat{(\phi_N^n)_l}(0) + \dfrac{\sin(\mu_l\tau)}{\mu_l}\widehat{(\phi_N^n)_l}'(0) - \widehat{(F_N^n)_l}, \\ \widehat{(\phi_N^n)_l}'(\tau) = -\mu_l\sin(\mu_l\tau)\widehat{(\phi_N^n)_l}(0) + \cos(\mu_l\tau)\widehat{(\phi_N^n)_l}'(0) - \widehat{(\dot{F}_N^n)_l}, \end{cases} \tag{3.13}$$

where

$$\widehat{(F_N^n)_l} = \mu_l \int_0^\tau \sin\left(\mu_l(\tau-\theta)\right)\left[e^{2i\theta/\varepsilon^2}\widehat{\left((z_N^n)^2\right)_l}(\theta) + e^{-2i\theta/\varepsilon^2}\widehat{\left((\overline{z_N^n})^2\right)_l}(\theta) + \widehat{(g_N^n)_l}(\theta)\right]d\theta, \tag{3.14a}$$

$$\widehat{(\dot{F}_N^n)_l} = \mu_l^2 \int_0^\tau \cos\left(\mu_l(\tau-\theta)\right)\left[e^{2i\theta/\varepsilon^2}\widehat{\left((z_N^n)^2\right)_l}(\theta) + e^{-2i\theta/\varepsilon^2}\widehat{\left((\overline{z_N^n})^2\right)_l}(\theta) + \widehat{(g_N^n)_l}(\theta)\right]d\theta, \tag{3.14b}$$

with

$$g_N^n(x,\theta) := 2e^{i\theta/\varepsilon^2}\left(z_N^n r_N^n\right) + 2e^{-i\theta/\varepsilon^2}\left(\overline{z_N^n} r_N^n\right) + 2|z_N^n|^2 + (r_N^n)^2.$$

Approximating the integrals in (3.13) and (3.14) either by the Gautschi's type quadrature [6,17,22,23] or by the single step trapezoidal rule [6,15,23], e.g. via the standard single step trapezoidal rule to the integrals involving r^n in (3.13) and g_N^n in (3.14) and via the Gautschi's type quadrature to the rest, noting $\widehat{(r_N^n\phi_N^n)_l}(0) = 0$ for $1 \le l \le N-1$ due to the initial data $r^n(x,0) \equiv 0$ for $a \le x \le b$ in (3.3), we get

$$
\begin{cases}
\widehat{(z_N^n)}_l(\tau) \approx a_l(\tau)\widehat{(z_N^n)}_l(0) + \varepsilon^2 b_l(\tau)\widehat{(z_N^n)}_l'(0) - c_l\widehat{(z_N^n\phi_N^n)}_l(0) - d_l\widehat{(z_N^n\phi_N^n)}_l'(0),\\
\widehat{(z_N^n)}_l'(\tau) \approx a_l'(\tau)\widehat{(z_N^n)}_l(0) + \varepsilon^2 b_l'(\tau)\widehat{(z_N^n)}_l'(0) - \dot{c}_l\widehat{(z_N^n\phi_N^n)}_l(0) - \dot{d}_l\widehat{(z_N^n\phi_N^n)}_l'(0),\\
\widehat{(r_N^n)}_l(\tau) \approx \dfrac{\sin(\omega_l\tau)}{\omega_l}\widehat{(r_N^n)}_l'(0), \qquad \widehat{(r_N^n)}_l'(\tau) \approx \cos(\omega_l\tau)\widehat{(r_N^n)}_l'(0) - \dfrac{\tau}{2\varepsilon^2}\widehat{(r_N^n\phi_N^n)}_l(\tau),\\
\widehat{(F_N^n)}_l \approx p_l\widehat{((z_N^n)^2)}_l(0) + q_l\widehat{((z_N^n)^2)}_l'(0) + \overline{p_l}\widehat{\left((\overline{z_N^n})^2\right)}_l(0) + \overline{q_l}\widehat{\left((\overline{z_N^n})^2\right)}_l'(0) + \tau\mu_l\sin(\mu_l\tau)\widehat{(|z_N^n|^2)}_l(0),\\
\widehat{(\dot{F}_N^n)}_l \approx \dot{p}_l\widehat{((z_N^n)^2)}_l(0) + \dot{q}_l\widehat{((z_N^n)^2)}_l'(0) + \overline{\dot{p}_l}\widehat{\left((\overline{z_N^n})^2\right)}_l(0) + \overline{\dot{q}_l}\widehat{\left((\overline{z_N^n})^2\right)}_l'(0) + \tau\mu_l^2\Big[\cos(\mu_l\tau)\widehat{(|z_N^n|^2)}_l(0)\\
\qquad + \widehat{(|z_N^n|^2)}_l(\tau) + \dfrac{1}{2}\widehat{(|r_N^n|^2)}_l(\tau) + \left(e^{i\tau/\varepsilon^2}\widehat{(z_N^n r_N^n)}_l(\tau) + e^{-i\tau/\varepsilon^2}\widehat{\left(\overline{z_N^n} r_N^n\right)}_l(\tau)\right)\Big],
\end{cases}
\tag{3.15}
$$

where $Re\{z\}$ denotes the real part of z and (their detailed explicit formulas are shown in Appendix A)

$$
\begin{cases}
c_l = \displaystyle\int_0^\tau b_l(\tau-\theta)\,d\theta, \qquad p_l = \mu_l\int_0^\tau \sin\left(\mu_l(\tau-\theta)\right)e^{2i\theta/\varepsilon^2}\,d\theta, \qquad d_l = \int_0^\tau b_l(\tau-\theta)\theta\,d\theta,\\
q_l = \mu_l\displaystyle\int_0^\tau \sin\left(\mu_l(\tau-\theta)\right)e^{2i\theta/\varepsilon^2}\theta\,d\theta, \qquad \dot{c}_l = \int_0^\tau b_l'(\tau-\theta)\,d\theta, \qquad \dot{d}_l = \int_0^\tau b_l'(\tau-\theta)\theta\,d\theta,\\
\dot{p}_l = \mu_l^2\displaystyle\int_0^\tau \cos\left(\mu_l(\tau-\theta)\right)e^{2i\theta/\varepsilon^2}\,d\theta, \qquad \dot{q}_l = \mu_l^2\int_0^\tau \cos\left(\mu_l(\tau-\theta)\right)e^{2i\theta/\varepsilon^2}\theta\,d\theta.
\end{cases}
\tag{3.16}
$$

Inserting (3.15) into (3.6) with setting $s=\tau$, and noticing (2.9), we immediately obtain a multiscale time integrator sine spectral method based on the MDF (3.2) for the problem (3.1).

In practice, the integrals for computing the sine transform coefficients in (3.5), (3.10) and (3.12) are usually approximated by the numerical quadratures [4,5,21,31] given in (3.5). Let ψ_j^n, $\dot{\psi}_j^n$, ϕ_j^n and $\dot{\phi}_j^n$ be approximations of $\psi(x_j,t_n)$, $\partial_t\psi(x_j,t_n)$, $\phi(x_j,t_n)$ and $\partial_t\phi(x_j,t_n)$, respectively; z_j^{n+1}, $\dot{z}_j^{n+1}$, r_j^{n+1} and $\dot{r}_j^{n+1}$ be approximations of $z^n(x_j,\tau)$, $\partial_s z^n(x_j,\tau)$, $r^n(x_j,\tau)$ and $\partial_s r^n(x_j,\tau)$, respectively, for $j=0,1,\ldots,N$. Choosing $\psi_j^0=\psi_0(x_j)$, $\dot{\psi}_j^0=\dfrac{1}{\varepsilon^2}\psi_1(x_j)$, $\phi_j^0=\phi_0(x_j)$ and $\dot{\phi}_j^0=\phi_1(x_j)$ for $0\le j\le N$, then a multiscale time integrator sine pseudospectral (MTI-SP) discretization for the problem (3.1) reads:

$$
\begin{cases}
\psi_j^{n+1} = 2Re\left\{e^{i\tau/\varepsilon^2}z_j^{n+1}\right\} + r_j^{n+1}, \qquad \dot{\psi}_j^{n+1} = 2Re\left\{e^{i\tau/\varepsilon^2}\left(\dot{z}_j^{n+1} + \dfrac{i}{\varepsilon^2}z_j^{n+1}\right)\right\} + \dot{r}_j^{n+1},\\
\phi_j^{n+1} = \displaystyle\sum_{l=1}^{N-1}\widetilde{(\phi^{n+1})}_l\sin(\mu_l(x_j-a)), \quad \dot{\phi}_j^{n+1} = \sum_{l=1}^{N-1}\widetilde{(\dot{\phi}^{n+1})}_l\sin(\mu_l(x_j-a)),\\
z_j^{n+1} = \displaystyle\sum_{l=1}^{N-1}\widetilde{(z^{n+1})}_l\sin(\mu_l(x_j-a)), \quad r_j^{n+1} = \sum_{l=1}^{N-1}\widetilde{(r^{n+1})}_l\sin(\mu_l(x_j-a)),\\
\dot{z}_j^{n+1} = \displaystyle\sum_{l=1}^{N-1}\widetilde{(\dot{z}^{n+1})}_l\sin(\mu_l(x_j-a)), \quad \dot{r}_j^{n+1} = \sum_{l=1}^{N-1}\widetilde{(\dot{r}^{n+1})}_l\sin(\mu_l(x_j-a)), \quad 0\le j\le N,\ n\ge 0,
\end{cases}
\tag{3.17}
$$

where

$$\widetilde{(z^{n+1})}_l = a_l(\tau)\widetilde{(z^0)}_l + \varepsilon^2 b_l(\tau)\widetilde{(\dot{z}^0)}_l - c_l\widetilde{(z^0\phi^n)}_l - d_l\widetilde{(\dot{z}^0\phi^n)}_l - d_l\widetilde{(z^0\dot{\phi}^n)}_l, \tag{3.18a}$$

$$\widetilde{(\dot{z}^{n+1})}_l = a_l'(\tau)\widetilde{(z^0)}_l + \varepsilon^2 b_l'(\tau)\widetilde{(\dot{z}^0)}_l - \dot{c}_l\widetilde{(z^0\phi^n)}_l - \dot{d}_l\widetilde{(\dot{z}^0\phi^n)}_l - \dot{d}_l\widetilde{(z^0\dot{\phi}^n)}_l, \tag{3.18b}$$

$$\widetilde{(r^{n+1})}_l = \frac{\sin(\omega_l\tau)}{\omega_l}\widetilde{(\dot{r}^0)}_l, \qquad \widetilde{(\dot{r}^{n+1})}_l = \cos(\omega_l\tau)\widetilde{(\dot{r}^0)}_l - \frac{\tau}{2\varepsilon^2}\widetilde{(r^{n+1}\phi^{n+1})}_l, \qquad 1\le l\le N-1, \tag{3.18c}$$

$$\widetilde{(\phi^{n+1})}_l = \cos(\mu_l\tau)\widetilde{(\phi^n)}_l + \frac{\sin(\mu_l\tau)}{\mu_l}\widetilde{(\dot{\phi}^n)}_l - \widetilde{(\mathcal{F}^n)}_l, \quad \widetilde{(\dot{\phi}^{n+1})}_l = -\mu_l\sin(\mu_l\tau)\widetilde{(\phi^n)}_l + \cos(\mu_l\tau)\widetilde{(\dot{\phi}^n)}_l - \widetilde{(\dot{\mathcal{F}}^n)}_l, \tag{3.18d}$$

with

$$\widetilde{(z^0)}_l = \frac{1}{2}\left[\widetilde{(\psi^n)}_l - i\varepsilon^2\widetilde{(\dot{\psi}^n)}_l\right], \qquad \widetilde{(\dot{z}^0)}_l = \frac{i}{2}\left[\frac{1}{\tau}\sin\left(\mu_l^2\tau\right)\widetilde{(z^0)}_l + \widetilde{(z^0\phi^n)}_l\right], \tag{3.19a}$$

$$\widetilde{(\dot{r}^0)}_l = -2Re\left\{\widetilde{(\dot{z}^0)}_l\right\}, \qquad \widetilde{(\mathcal{F}^n)}_l = 2Re\left\{p_l\widetilde{((z^0)^2)}_l + 2q_l\widetilde{(z^0\dot{z}^0)}_l\right\} + \tau\mu_l\sin(\mu_l\tau)\widetilde{(|z^0|^2)}_l, \tag{3.19b}$$

$$\begin{aligned}\widetilde{(\dot{\mathcal{F}}^n)}_l = {} & 2Re\left\{\dot{p}_l\widetilde{((z^0)^2)}_l + 2\dot{q}_l\widetilde{(z^0\dot{z}^0)}_l\right\} + \tau\mu_l^2\left[e^{i\tau/\varepsilon^2}\widetilde{(z^{n+1}r^{n+1})}_l + e^{-i\tau/\varepsilon^2}\widetilde{\left(\overline{z^{n+1}}r^{n+1}\right)}_l\right] \\ & + \tau\mu_l^2\left[\cos(\mu_l\tau)\widetilde{(|z^0|^2)}_l + \widetilde{(|z^{n+1}|^2)}_l + \frac{1}{2}\widetilde{(|r^{n+1}|^2)}_l\right], \qquad 1 \le l \le N-1.\end{aligned} \tag{3.19c}$$

This MTI-SP method for the KGZ system (3.1) (or (1.3) with (1.5)) is explicit, accurate, easy to be implemented and very efficient due to the fast discrete sine transform. The memory cost is $O(N)$ and the computational cost per time step is $O(N\log N)$.

Remark 3.1. Instead of discretizing the initial velocity $\partial_s z^n(x,0)$ from (3.3) in the Fourier space as $\widetilde{(z^n)}_l'(0) = \frac{i}{2}[\mu_l^2\widetilde{(z^n)}_l(0) + \widetilde{(z^n\phi^n)}_l(0)]$ which will result a second order decreasing in the spatial accuracy, we change to the modified coefficients given in (3.19a) as filters where the accuracy is now controlled by the time step τ [3]. There are other possible choices of the filters.

Remark 3.2. We remark here that the proposed MTI-SP method for the KGZ system (1.3) can be extended to solve the generalized KGZ system with pure power nonlinearities [24,34]

$$\varepsilon^2\partial_{tt}\psi(\mathbf{x},t) - \Delta\psi(\mathbf{x},t) + \frac{1}{\varepsilon^2}\psi(\mathbf{x},t) + p\phi(\mathbf{x},t)\psi^{2p-1}(\mathbf{x},t) + \lambda\psi^{2q}(\mathbf{x},t)\psi(\mathbf{x},t) = 0, \tag{3.20a}$$

$$\partial_{tt}\phi(\mathbf{x},t) - \Delta\phi(\mathbf{x},t) - \Delta\left(\psi^{2p}(\mathbf{x},t)\right) = 0, \qquad \mathbf{x}\in\mathbb{R}^d, \tag{3.20b}$$

where $p\in\mathbb{N}$, $q\in\mathbb{N}$ and $\lambda\in\mathbb{R}$. The extension of the EWI-SP to solve (3.20b) is straightforward. To integrate the power nonlinearity in (3.20a), the MTI-SP which could provide a uniform error bound for $0<\varepsilon\le 1$, can be designed by following the way used in [3]. Also, our method can be easily extended to the cases when the homogeneous Dirichlet boundary condition is replaced by the homogeneous Neumann or periodic boundary condition in order to deal with special physical situations such as the dark solitons [34], via replacing the discrete sine transform in the MTI-SP method by the discrete cosine or Fourier transform.

Remark 3.3. When the initial data $\psi_0(x)$ and $\psi_1(x)$ in (1.5) are taken as complex-valued functions, the component $\psi(x,t)$ in the KGZ system (1.3a) is complex-valued, which has been widely considered in the literatures on mathematical analysis and solitary wave prorogations of the KGZ system [10,24,26,35,34]. In this case, for $n\ge 0$, we modify the ansatz (2.2) to [3,9]

$$\psi(\mathbf{x},t_n+s) = e^{is/\varepsilon^2}z_+^n(\mathbf{x},s) + e^{-is/\varepsilon^2}\overline{z_-^n}(\mathbf{x},s) + r^n(\mathbf{x},s), \qquad \mathbf{x}\in\mathbb{R}^d, \qquad 0\le s\le\tau,$$

where $z_\pm^n$ are two different complex-valued functions. Similar to the nonlinear KG equation [3], we can obtain a MDF for the KGZ system where the first equation in (2.4) will be replaced by a system of two coupled equations with unknowns $z_\pm^n$. Then the MTI-SP method can be designed straightforward.

4. Numerical results

In this section, we present numerical results of the MTI-SP method including spatial/temporal accuracy, ε-scalability when $0<\varepsilon\ll 1$, and its applications to study numerically convergence rates of the KGZ system to its limiting models when $\varepsilon\to 0$, interactions of solitons in 1D, parameter regimes of finite time blow-up in 1D and wave interactions in 2D.

4.1. Spatial/temporal accuracy and ε-scalability

In order to do so, we take $d=1$ in (1.3) and choose the initial data in (1.5) as

$$\psi_0(x) = e^{-\frac{x^2}{2}}, \quad \psi_1(x) = \frac{3}{2}\psi_0(x), \quad \phi_0(x) = \operatorname{sech}(x^2), \quad \phi_1(x) = 0, \qquad x\in\mathbb{R}. \tag{4.1}$$

Table 1
Spatial errors of the MTI-SP for the KGZ with (4.1) under $\tau = 5 \times 10^{-6}$ for different ε and h.

$e_\phi(T=1)$	$h_0=2$	$h_0/2$	$h_0/4$	$h_0/8$	$h_0/16$
$\varepsilon_0 = 0.5$	5.43E–1	3.84E–2	7.85E–4	1.53E–7	8.36E–12
$\varepsilon_0/2$	5.70E–1	3.79E–2	2.00E–3	1.49E–7	7.51E–12
$\varepsilon_0/2^2$	5.85E–1	3.72E–2	2.10E–3	8.49E–8	7.53E–12
$\varepsilon_0/2^3$	5.90E–1	3.69E–2	2.10E–3	8.14E–8	7.39E–12
$\varepsilon_0/2^4$	5.91E–1	3.68E–2	2.10E–3	8.05E–8	7.44E–12
$\varepsilon_0/2^5$	5.91E–1	3.67E–2	2.10E–3	8.02E–8	7.43E–12
$\varepsilon_0/2^7$	5.91E–1	3.68E–2	2.10E–3	8.01E–8	7.40E–12
$\varepsilon_0/2^9$	5.91E–1	3.68E–2	2.10E–3	8.01E–8	7.46E–12
$\varepsilon_0/2^{11}$	5.91E–1	3.68E–2	2.10E–3	8.01E–8	7.54E–12
$\varepsilon_0/2^{13}$	5.91E–1	3.68E–2	2.10E–3	8.01E–8	7.42E–12

$e_\psi(T=1)$	$h_0=2$	$h_0/2$	$h_0/4$	$h_0/8$	$h_0/16$
$\varepsilon_0 = 0.5$	4.22E–1	1.07E–1	2.40E–3	9.23E–8	5.77E–11
$\varepsilon_0/2$	5.34E–1	1.29E–1	2.10E–3	2.13E–7	3.68E–11
$\varepsilon_0/2^2$	5.03E–1	2.25E–1	1.90E–3	2.20E–7	3.36E–11
$\varepsilon_0/2^3$	3.71E–1	2.17E–1	2.10E–3	4.27E–7	3.94E–11
$\varepsilon_0/2^4$	4.94E–1	1.03E–1	7.70E–4	1.62E–7	4.21E–11
$\varepsilon_0/2^5$	2.92E–1	7.52E–2	1.00E–3	4.06E–7	4.62E–11
$\varepsilon_0/2^7$	2.38E–1	9.20E–2	1.20E–3	3.58E–7	4.99E–11
$\varepsilon_0/2^9$	6.17E–1	1.87E–1	1.80E–3	1.72E–7	3.90E–11
$\varepsilon_0/2^{11}$	1.95E–1	1.14E–1	1.40E–3	3.70E–7	3.91E–11
$\varepsilon_0/2^{13}$	4.28E–1	2.33E–1	2.50E–3	3.72E–7	4.71E–11

The problem is solved numerically by the MTI-SP method on a bounded interval $\Omega = [-16, 16]$, i.e. $b = -a = 16$, which is large enough to guarantee that the zero boundary condition does not introduce a significant truncation error relative to the original problem. To quantify the error, we introduce the error functions:

$$e_\psi(T) := \left\| \psi(\cdot, T) - I_N(\psi^M) \right\|_{H^2}, \qquad e_\psi^\infty(T) := \max_{0<\varepsilon\le 1} \left\{ e_\psi(T) \right\}, \tag{4.2a}$$

$$e_\phi(T) := \left\| \phi(\cdot, T) - I_N(\phi^M) \right\|_{H^1}, \qquad e_\phi^\infty(T) := \max_{0<\varepsilon\le 1} \left\{ e_\phi(T) \right\}, \tag{4.2b}$$

where $\psi^M = (\psi_0^M, \psi_1^M, \ldots, \psi_N^M)^T$ and $\phi^M = (\phi_0^M, \phi_1^M, \ldots, \phi_N^M)^T$ are obtained numerically from the MTI-SP (3.17)–(3.19) with $T = M\tau$. The reason why here we choose the energy space $H^2 \times H^1$ rather than the natural $H^1 \times L^2$ for the errors is because an H^2-estimate is needed for an optimal error estimate of the nonlinear KG equation [3]. Since the analytical solution to this problem is not available, so the 'reference' solution is obtained numerically by the MTI-SP (3.17)–(3.19) with a very fine mesh $h = 1/32$ and a very small time step $\tau = 5 \times 10^{-6}$. Table 1 shows the spatial error of the MTI-SP method at $T = 1$ under different ε and h with the time step $\tau = 5 \times 10^{-6}$ such that the discretization error in time is negligible. Tables 2 and 3 show the temporal error of the MTI-SP method for components ϕ and ψ, respectively, at $T = 1$ under different ε and τ with a small mesh size $h = 1/8$ such that the discretization error in space is negligible.

From Tables 1–3, we can draw the following observations:

(i) The MTI-SP method is spectrally accurate in space, which is uniformly for $0 < \varepsilon \le 1$ (cf. Table 1).

(ii) The MTI-SP method converges uniformly for $\varepsilon \in (0, 1]$ at linear convergence rate in time (cf. last row in Tables 2 and 3). In addition, for each fixed $\varepsilon \in (0, 1]$, it converges quadratically in time when either $0 < \tau \lesssim \varepsilon^2$ (cf. each row in the upper triangle above the diagonal labeled with bold letters of Tables 2 and 3) or $0 < \varepsilon \lesssim \tau$ (cf. each row in the lower triangle below the diagonal labeled with italic letters of Tables 2 and 3).

(iii) The numerical results indicate the following error bounds of the MTI-SP method for the KGZ system (1.3) with $\varepsilon \in (0, 1]$

$$e_\psi(t_n) + e_\phi(t_n) \lesssim h^{m_0} + \frac{\tau^2}{\varepsilon^2}, \qquad e_\psi(t_n) + e_\phi(t_n) \lesssim h^{m_0} + \tau^2 + \varepsilon^2, \qquad 0 \le n \le \frac{T}{\tau}, \tag{4.3}$$

which immediately imply the following uniform error bound

$$e_\psi(t_n) + e_\phi(t_n) \lesssim h^{m_0} + \min\left\{ \frac{\tau^2}{\varepsilon^2}, \tau^2 + \varepsilon^2 \right\} \lesssim h^{m_0} + \tau, \qquad 0 \le n \le \frac{T}{\tau},$$

with $m_0 > 0$ depending on the regularity of the solution. Rigorous mathematical justification for the above error estimates of the MTI-SP method is on-going. In fact, the above error bounds of the MTI-SP method have been established for the nonlinear KG equation [3] and the KGS equations [9].

(iv) The mesh strategy (or ε-scalability) of the MTI-SP method for the KGZ system (1.3) in the high-plasma-frequency limit regime, i.e. $0 < \varepsilon \ll 1$, is $\tau = O(1)$ and $h = O(1)$.

Table 2
Temporal errors $e_\phi(T=1)$ of the MTI-SP for the KGZ with (4.1) under $h=1/8$ for different ε and τ.

$e_\phi(T=1)$	$\tau_0=0.2$	$\tau_0/2^2$	$\tau_0/2^4$	$\tau_0/2^6$	$\tau_0/2^8$	$\tau_0/2^{10}$	$\tau_0/2^{12}$
$\varepsilon_0=0.5$	1.41E−1	**1.16E−2**	6.85E−4	4.19E−5	2.60E−6	1.60E−7	7.37E−9
Rate	—	**1.80**	2.04	2.02	2.00	2.01	2.21
$\varepsilon_0/2$	4.08E−2	2.92E−2	**2.10E−3**	1.22E−4	7.51E−6	4.60E−7	2.14E−8
Rate	—	0.24	**1.90**	2.05	2.01	2.01	2.21
$\varepsilon_0/2^2$	3.81E−2	1.55E−2	6.80E−3	**4.63E−4**	2.75E−5	1.66E−6	7.77E−8
Rate	—	0.65	0.59	**1.94**	2.04	2.02	2.21
$\varepsilon_0/2^3$	*5.25E−2*	4.40E−3	6.70E−3	1.70E−3	**1.12E−4**	6.58E−6	3.03E−7
Rate	—	1.79	−0.30	0.99	**1.96**	2.05	2.21
$\varepsilon_0/2^4$	5.29E−2	2.60E−3	1.80E−3	1.90E−3	4.12E−4	**2.75E−5**	1.23E−6
Rate	—	2.17	0.26	−0.04	1.10	**1.95**	2.24
$\varepsilon_0/2^5$	5.31E−2	*3.00E−3*	1.22E−4	4.92E−4	4.86E−4	1.01E−4	**5.19E−6**
Rate	—	*2.07*	2.31	−1.01	0.01	1.13	**2.14**
$\varepsilon_0/2^7$	5.38E−2	3.40E−3	*1.95E−4*	2.53E−5	2.59E−5	4.05E−5	3.95E−5
Rate	—	1.99	*2.06*	1.47	−0.02	−0.32	0.02
$\varepsilon_0/2^9$	5.39E−2	3.40E−3	2.10E−4	*1.21E−5*	1.09E−6	9.34E−7	3.38E−7
Rate	—	1.99	2.01	*2.06*	1.73	0.11	0.73
$\varepsilon_0/2^{11}$	5.39E−2	3.40E−3	2.11E−4	1.31E−5	*7.14E−7*	8.43E−8	3.33E−8
Rate	—	1.99	2.00	2.00	*2.10*	1.54	0.67
$\varepsilon_0/2^{13}$	5.39E−2	3.40E−3	2.11E−4	1.31E−5	8.24E−7	*5.75E−8*	2.42E−9
Rate	—	1.99	2.01	2.00	2.00	*1.92*	2.28
$\varepsilon_0/2^{15}$	5.42E−2	3.40E−3	2.14E−4	1.33E−5	8.32E−7	5.13E−8	*2.47E−9*
Rate	—	2.00	1.99	2.00	2.00	2.01	*2.18*
$e_\phi^\infty(T=1)$	1.41E−1	2.92E−2	6.80E−3	1.90E−3	4.86E−4	1.01E−4	3.95E−5
Rate	—	1.13	1.05	0.92	0.98	1.13	0.68

Table 3
Temporal errors $e_\psi(T=1)$ of the MTI-SP for the KGZ with (4.1) under $h=1/8$ for different ε and τ.

$e_\psi(T=1)$	$\tau_0=0.2$	$\tau_0/2^2$	$\tau_0/2^4$	$\tau_0/2^6$	$\tau_0/2^8$	$\tau_0/2^{10}$	$\tau_0/2^{12}$
$\varepsilon_0=0.5$	4.52E−2	**4.10E−3**	2.62E−4	1.63E−5	1.02E−6	6.26E−8	2.86E−9
Rate	—	**1.73**	1.99	2.00	2.00	2.01	2.22
$\varepsilon_0/2$	6.66E−2	1.28E−2	**1.10E−3**	6.74E−5	4.20E−6	2.58E−7	1.20E−8
Rate	—	1.19	**1.77**	2.01	2.00	2.01	2.21
$\varepsilon_0/2^2$	6.35E−2	1.66E−2	4.00E−3	**3.18E−4**	1.99E−5	1.22E−6	5.71E−8
Rate	—	0.97	1.03	**1.83**	2.00	2.01	2.20
$\varepsilon_0/2^3$	*5.88E−2*	7.80E−3	5.00E−3	9.82E−4	**7.73E−5**	4.77E−6	2.23E−7
Rate	—	1.46	0.32	1.17	**1.83**	2.01	2.20
$\varepsilon_0/2^4$	6.66E−2	4.30E−3	1.30E−3	1.20E−3	2.11E−4	**1.64E−5**	7.80E−7
Rate	—	1.98	0.86	0.06	1.25	**1.84**	2.19
$\varepsilon_0/2^5$	6.34E−2	*4.10E−3*	3.61E−4	2.95E−4	2.95E−4	4.85E−5	**2.92E−6**
Rate	—	*1.98*	1.75	0.15	0.00	1.30	**2.02**
$\varepsilon_0/2^7$	6.21E−2	3.90E−3	*2.51E−4*	3.19E−5	1.48E−5	1.98E−5	1.98E−5
Rate	—	1.99	*1.98*	1.49	0.55	−0.21	0.00
$\varepsilon_0/2^9$	6.80E−2	4.10E−3	2.56E−4	*1.65E−5*	1.32E−6	7.10E−7	2.15E−7
Rate	—	2.02	2.00	*1.98*	1.82	0.45	0.86
$\varepsilon_0/2^{11}$	6.11E−2	3.80E−3	2.39E−4	1.50E−5	*9.95E−7*	1.30E−7	4.70E−8
Rate	—	2.00	1.99	2.00	*1.96*	1.47	0.73
$\varepsilon_0/2^{13}$	6.11E−2	3.80E−3	2.38E−4	1.49E−5	9.27E−7	*5.70E−8*	7.76E−9
Rate	—	2.00	2.00	2.00	2.00	*2.01*	1.45
$\varepsilon_0/2^{15}$	8.04E−2	4.90E−3	3.01E−4	1.87E−5	1.08E−6	7.01E−8	*6.32E−9*
Rate	—	2.01	2.01	2.00	2.05	1.97	*1.74*
$e_\psi^\infty(T=1)$	6.66E−2	1.66E−2	5.00E−3	1.20E−3	2.95E−4	4.85E−5	1.98E−5
Rate	—	1.00	0.87	1.02	1.01	1.30	0.65

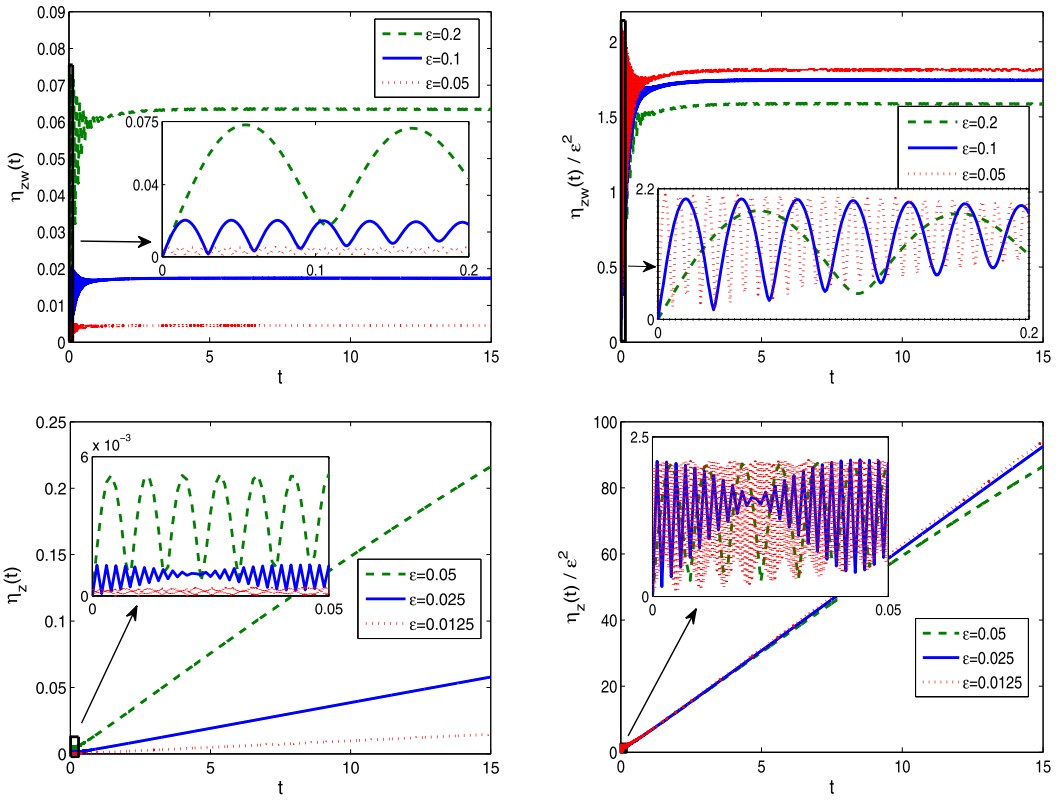

Fig. 2. Time evolution of $\eta_{zw}(t)$ and $\eta_z(t)$ with the smooth data (4.4) for different ε.

4.2. Convergence rates of the KGZ system to its limiting models when $\varepsilon \to 0$

In order to do so, we take $d = 1$ in (1.3) and choose the initial data in (1.5) as either the smooth data

$$\psi_0(x) = \sin\left(\frac{x}{2}\right) e^{-x^2}, \quad \psi_1(x) = \frac{1}{2} e^{-\sqrt{2}x^2}, \quad \phi_0(x) = \operatorname{sech}(x^2), \quad \phi_1(x) = \cos\left(\frac{x}{3}\right) e^{-x^2}, \qquad x \in \mathbb{R}, \tag{4.4}$$

or the nonsmooth data with $m = 2, 1$

$$\psi_0(x) = \frac{x^m |x|}{2} e^{-x^2}, \quad \psi_1(x) = \frac{1}{2} e^{-\sqrt{2}x^2}, \quad \phi_0(x) = x^m |x| \operatorname{sech}(x^2), \quad \phi_1(x) = \cos\left(\frac{x}{3}\right) e^{-x^2}, \quad x \in \mathbb{R}. \tag{4.5}$$

Let (ψ, ϕ) be the solution of the KGZ system (1.3) with either (4.4) or (4.5) which is obtained numerically by the MTI-SP method (3.17)–(3.19) on a bounded interval $\Omega = [-128, 128]$ with a very fine mesh $h = 1/32$ and a very small time step $\tau = 10^{-4}$. Similarly, let (z_{zw}, ϕ_{zw}) be the solution of the Zakharov system with wave operator (1.8) with $d = 1$ and (1.9), which is obtained numerically on the bounded interval Ω by the EWI-SP method proposed in [2] with a very fine mesh $h = 1/128$ and a very small time step $\tau = 10^{-4}$; and (z_z, ϕ_z) be the solution of the Zakharov system (1.10) with $d = 1$ and (1.11), which is obtained numerically on the bounded interval Ω by the time-splitting exponential wave integrator sine pseudospectral (TS-EWI-SP) method in [7,8] with a very fine mesh size $h = 1/128$ and a very small time step $\tau = 10^{-4}$. Denote

$$\psi_{zw}(x,t) = e^{it/\varepsilon^2} z_{zw}(x,t) + e^{-it/\varepsilon^2} \overline{z_{zw}}(x,t), \quad \psi_z(x,t) = e^{it/\varepsilon^2} z_z(x,t) + e^{-it/\varepsilon^2} \overline{z_z}(x,t), \quad x \in \mathbb{R}, \quad t \geq 0,$$

and define the error functions as

$$\eta_{zw}(t) := \|\psi(\cdot,t) - \psi_{zw}(\cdot,t)\|_{H^1} + \|\phi(\cdot,t) - \phi_{zw}(\cdot,t)\|_{L^2}, \quad \eta_z(t) := \|\psi(\cdot,t) - \psi_z(\cdot,t)\|_{H^1} + \|\phi(\cdot,t) - \phi_z(\cdot,t)\|_{L^2}.$$

Figs. 2 and 3 depict $\eta_{zw}(t)$ and $\eta_z(t)$ with the smooth data (4.4) and the nonsmooth data (4.5) with $m = 2, 1$, respectively, for different ε.

From Figs. 2 and 3, we can draw the following conclusions:

(i) The solution of the KGZ system (1.3) with (1.5) converges to that of its semi-limiting model, i.e. the Zakharov system with wave operator (1.8) with (1.9) quadratically in ε (and uniformly in time) provided that the initial data in (1.5) is smooth or at least satisfies ψ_0, ψ_1, ϕ_0 and $\phi_1 \in H^2(\mathbb{R}^d)$, i.e.

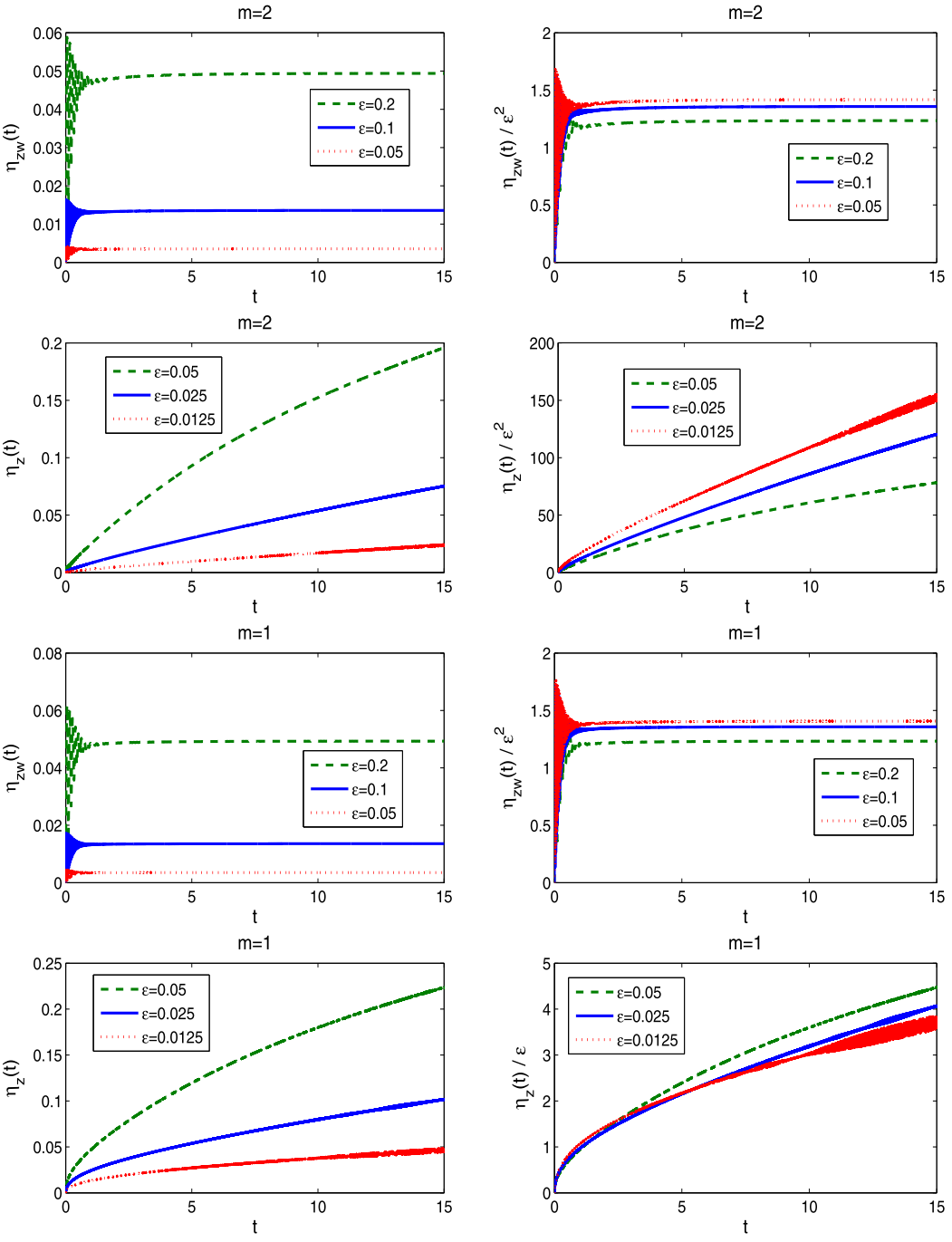

Fig. 3. Time evolution of $\eta_{zw}(t)$ and $\eta_z(t)$ with the nonsmooth data (4.5) under $m = 2, 1$ for different ε.

$$\|\psi(\cdot,t) - \psi_{zw}(\cdot,t)\|_{H^1(\Omega)} + \|\phi(\cdot,t) - \phi_{zw}(\cdot,t)\|_{L^2(\Omega)} \le C_0\varepsilon^2, \qquad t \ge 0,$$

where the constant $C_0 > 0$ is independent of ε and time $t \ge 0$.

(ii) The solution of the KGZ system (1.3) with (1.5) converges to that of its limiting model, i.e. the Zakharov system (1.10) with (1.11) quadratically in ε (in general, not uniformly in time) provided that the initial data in (1.5) is smooth or at least satisfies ψ_0, ψ_1, ϕ_0 and $\phi_1 \in H^3(\mathbb{R}^d)$, i.e.

$$\|\psi(\cdot,t) - \psi_z(\cdot,t)\|_{H^1(\Omega)} + \|\phi(\cdot,t) - \phi_z(\cdot,t)\|_{L^2(\Omega)} \le (C_1 + C_2 T)\varepsilon^2, \qquad 0 \le t \le T,$$

where C_1 and C_2 are two positive constants which are independent of ε and T. On the contrary, if the regularity of the initial data is weaker, e.g. ψ_0, ψ_1, ϕ_0 and $\phi_1 \in H^2(\mathbb{R}^d)$, then the convergence rate reduces to linear rate, i.e.

$$\|\psi(\cdot,t)-\psi_z(\cdot,t)\|_{H^1(\Omega)}+\|\phi(\cdot,t)-\phi_z(\cdot,t)\|_{L^2(\Omega)}\le(C_3+C_4T)\varepsilon,\quad 0\le t\le T,$$

where C_3 and C_4 are two positive constants which are independent of ε and T. Again, rigorous mathematical justification for these numerical observations is on-going.

4.3. Soliton solutions and their stability and interactions

It is well-known that the KGZ system (1.3) in 1D admits the bright soliton solution as [34]

$$\psi^s(x,t;\alpha,k)=\alpha\,\mathrm{sech}(B(x-vt))e^{i(\omega t-kx)},\quad \phi^s(x,t;\alpha,k)=A\,\mathrm{sech}^2(B(x-vt)),\quad x\in\mathbb{R},\ t>0, \tag{4.6}$$

where the coefficients $A, B, \omega, v\in\mathbb{R}$ satisfy

$$A=\frac{\varepsilon^4\omega^2\alpha^2}{k^2-\varepsilon^4\omega^2},\quad v=\frac{k}{\varepsilon^2\omega},\quad B=\omega\sqrt{\frac{1+\varepsilon^2k^2-\varepsilon^4\omega^2}{\varepsilon^2\omega^2-k^2}}, \tag{4.7a}$$

$$2\varepsilon^4\omega^4+\left(\varepsilon^2\alpha^2-2k^2-2k^2\varepsilon^2-2\right)\omega^2+2k^4\varepsilon^{-2}+2k^2\varepsilon^{-4}=0, \tag{4.7b}$$

with $\alpha, k\in\mathbb{R}$ two free parameters. Equation (4.7b) has roots

$$\omega=\frac{1}{2\varepsilon^2}\sqrt{-\sigma\pm\sqrt{\sigma^2-16(k^4\varepsilon^2+k^2)}}\quad\text{with}\quad \sigma=\varepsilon^2\alpha^2-2k^2-2k^2\varepsilon^2-2. \tag{4.8}$$

By assuming the two constants $|\alpha|\lesssim 1$ and $k=O(1)$ for $\varepsilon\in(0,1]$, noticing (4.8) and (4.7a), we get

$$\omega\varepsilon^2=\sqrt{\frac{k^2+1\pm|1-k^2|}{2}}+o(1),\quad B\varepsilon=\sqrt{\frac{1-k^2\mp|1-k^2|}{2}}+o(1),\qquad 0<\varepsilon\ll 1. \tag{4.9}$$

In order to find soliton solutions with wavelength at $O(1)$ in space, i.e. $B=O(1)$, for $\varepsilon\in(0,1]$, noticing (4.9), we have $k=\pm1$. Without loss of generality, we only consider the case of $k=1$. Under this choice, combining (4.7) and (4.8), we can derive a sufficient condition for the existence of the soliton for all $\varepsilon\in(0,1]$,

$$0<|\alpha|\le\frac{\sqrt{2}\varepsilon}{1+\sqrt{1+\varepsilon^2}},\qquad 0<\varepsilon\le 1.$$

For the simplicity of notations, we take $\alpha=\delta\varepsilon$ with $\delta\in\mathbb{R}$ a constant independent of ε and satisfying $|\delta|\le\frac{\sqrt{2}}{1+\sqrt{2}}$. Plugging $k=1$ and $\alpha=\delta\varepsilon$ into (4.7) and (4.8), when $0<\varepsilon\ll1$ we have

$$\omega=\varepsilon^{-2}+\frac{1\pm\sqrt{1-2\delta^2}}{4}+o(1)=O(\varepsilon^{-2}),\quad B=\sqrt{\frac{1\mp\sqrt{1-2\delta^2}}{2}}+o(1)=O(1),\quad A=O(1),\quad v=O(1).$$

From now on, we take

$$\omega=\frac{1}{2\varepsilon^2}\sqrt{-\sigma-\sqrt{\sigma^2-16(k^4\varepsilon^2+k^2)}}\,. \tag{4.10}$$

Thus, for proper given $\alpha=\delta\varepsilon$ and k with $\varepsilon>0$ and $\delta>0$, we can find ω from (4.10) and A, v and B from (4.7a) and thus we can obtain a soliton solution (4.6) of the KGZ system (1.3) in 1D.

Here we adapt the soliton solution to test again the spatial/temporal accuracy and ε-scalability of the proposed MTI-SP method. In order to do so, we take $d=1$ in (1.3) and choose the initial data in (1.5) as

$$\psi_0(x)=\psi^s(x,0;\alpha,k),\quad \psi_1(x)=\varepsilon^2\partial_t\psi^s(x,0;\alpha,k),\quad \phi_0(x)=\phi^s(x,0;\alpha,k),\quad \phi_1(x)=\partial_t\phi^s(x,0;\alpha,k), \tag{4.11}$$

where $\alpha=\dfrac{\varepsilon}{\sqrt{3}}$ and $k=1$. It is easy to see that the solution of the KGZ system (1.3) with $d=1$ and (4.11) satisfies $\psi=O(\varepsilon)$, $\partial_t\psi=O(\varepsilon^{-1})$ and $\phi=O(1)$ when $0<\varepsilon\ll1$, and thus this example is quite different with the example in §4.1. In fact, the initial data in (4.11) and (1.5) (or (4.1)) for the KGZ system (1.3) are quite different in at least two aspects: (i) the energy in (1.6) is unbounded, i.e. $E(t)=O(\varepsilon^{-2})$ for $0<\varepsilon\ll1$ for the initial data (1.5), while it is bounded, i.e. $E(t)=O(1)$ for $0<\varepsilon\le1$ for the initial data (4.11); and (ii) the solution $\psi=O(1)$ for the initial data (1.5), while it is small, i.e. $\psi=O(\varepsilon)$ for the initial data (4.11). Thus the initial data (1.5) is usually referred as *large initial data* or energy unbounded initial data when $\varepsilon\to0^+$, and respectively, the initial data (4.11) is usually referred as *small initial data* or energy bounded initial data. The problem is solved numerically on $\Omega=[-16,16]$ by either the MTI-SP method (3.17)–(3.19) or the EWI-SP method proposed in [5]. Here we adapt the relative error

Table 4
Temporal errors $\eta_\phi(T=1)$ of the MTI-SP for the KGZ with (4.11) under $h=1/8$ for different ε and τ.

$\eta_\phi(T=1)$	$\tau_0=0.2$	$\tau_0/2^2$	$\tau_0/2^4$	$\tau_0/2^6$	$\tau_0/2^8$	$\tau_0/2^{10}$	$\tau_0/2^{12}$
$\varepsilon_0=0.5$	3.80E–3	**1.89E–4**	1.07E–5	6.59E–7	4.10E–8	2.58E–9	1.56E–10
Rate	–	**2.16**	2.06	2.01	2.00	2.00	2.02
$\varepsilon_0/2$	2.95E–4	1.21E–4	**4.24E–6**	2.01E–7	1.17E–8	7.15E–10	3.77E–11
Rate	–	–	**2.41**	2.20	2.05	2.02	2.12
$\varepsilon_0/2^2$	5.64E–5	1.16E–5	6.45E–6	**2.03E–7**	8.74E–9	4.89E–10	3.59E–11
Rate	–	–	–	**2.49**	2.27	2.08	1.881
$\varepsilon_0/2^3$	1.28E–5	1.40E–6	6.18E–7	3.87E–7	**1.19E–8**	4.99E–10	3.64E–11
Rate	–	–	–	–	**2.51**	2.28	1.89
$\varepsilon_0/2^4$	3.12E–6	2.20E–7	6.25E–8	3.70E–8	2.40E–8	**7.33E–10**	3.91E–11
Rate	–	–	–	–	–	**2.52**	2.11
$\varepsilon_0/2^5$	7.73E–7	4.87E–8	6.23E–9	3.61E–9	2.29E–9	1.50E–9	**5.19E–11**
Rate	–	–	–	–	–	–	**2.42**
$\varepsilon_0/2^7$	4.83E–8	2.93E–9	1.81E–10	3.64E–11	3.03E–11	2.81E–11	2.65E–11
Rate	–	–	–	–	–	–	–
$\varepsilon_0/2^9$	3.04E–9	2.08E–10	5.49E–11	4.92E–11	4.89E–11	4.89E–11	4.90E–11
Rate	–	–	–	–	–	–	–
$\varepsilon_0/2^{11}$	8.79E–10	7.61E–10	7.53E–10	7.53E–10	7.53E–10	7.53E–10	7.53E–10
Rate	–	–	–	–	–	–	–
$\eta_\phi^\infty(T=1)$	3.80E–3	1.89E–4	1.07E–5	6.59E–7	4.10E–8	2.58E–9	1.56E–10
Rate	–	2.16	2.06	2.01	2.00	2.00	2.02

Table 5
Temporal errors $\eta_\psi(T=1)$ of the MTI-SP for the KGZ with (4.11) under $h=1/8$ for different ε and τ.

$\eta_\psi(T=1)$	$\tau_0=0.2$	$\tau_0/2^2$	$\tau_0/2^4$	$\tau_0/2^6$	$\tau_0/2^8$	$\tau_0/2^{10}$	$\tau_0/2^{12}$
$\varepsilon_0=0.5$	3.78E–2	**1.60E–3**	8.90E–5	5.44E–6	3.38E–7	2.10E–8	1.82E–9
Rate	–	**2.28**	2.08	2.02	2.00	2.00	1.77
$\varepsilon_0/2$	2.62E–2	3.60E–3	**2.13E–4**	1.32E–5	8.22E–7	5.09E–8	3.24E–9
Rate	–	1.43	**2.03**	2.00	2.00	2.00	1.99
$\varepsilon_0/2^2$	1.92E–2	4.10E–3	7.48E–4	**4.86E–5**	3.04E–6	1.87E–7	8.78E–9
Rate	–	1.11	1.23	**1.97**	2.00	2.01	2.20
$\varepsilon_0/2^3$	*1.74E–2*	1.80E–3	8.80E–4	1.81E–4	**1.19E–5**	7.36E–7	3.45E–8
Rate	–	1.63	0.52	1.14	**1.96**	2.01	2.20
$\varepsilon_0/2^4$	1.73E–2	1.10E–3	2.65E–4	2.17E–4	4.48E–5	**2.92E–6**	1.38E–7
Rate	–	1.99	1.03	0.14	1.14	**1.97**	2.20
$\varepsilon_0/2^5$	1.73E–2	*1.10E–3*	8.49E–5	5.66E–5	5.48E–5	1.10E–5	**5.48E–7**
Rate	–	*1.99*	1.85	0.29	0.02	1.16	**2.16**
$\varepsilon_0/2^7$	1.72E–2	1.10E–3	*6.76E–5*	7.24E–6	4.16E–6	4.40E–6	4.14E–6
Rate	–	1.99	*2.01*	1.61	2.01	−0.04	0.04
$\varepsilon_0/2^9$	1.72E–2	1.10E–3	6.61E–5	*4.27E–6*	3.82E–7	1.20E–7	3.56E–8
Rate	–	1.99	2.01	*1.98*	1.74	0.84	0.87
$\varepsilon_0/2^{11}$	2.06E–2	1.30E–3	7.87E–5	4.92E–6	*3.16E–7*	3.12E–8	1.07E–8
Rate	–	1.99	2.02	2.00	*1.98*	1.67	0.77
$\varepsilon_0/2^{13}$	7.30E–3	4.51E–4	3.03E–5	2.01E–6	1.28E–7	*1.14E–8*	3.17E–9
Rate	–	2.01	1.95	1.96	1.99	*1.74*	0.92
$\eta_\psi^\infty(T=1)$	3.78E–2	4.10E–3	8.80E–4	2.17E–4	5.48E–5	1.10E–5	4.14E–6
Rate	–	1.60	1.10	1.01	0.99	1.12	0.71

$$\eta_\psi(T)=\frac{e_\psi(T)}{\|\psi(\cdot,T)\|_{H^2}},\quad \eta_\phi(T)=\frac{e_\phi(T)}{\|\phi(\cdot,T)\|_{H^1}},\quad \eta_\psi^\infty(T)=\frac{e_\psi^\infty(T)}{\|\psi(\cdot,T)\|_{H^2}},\quad \eta_\phi^\infty(T)=\frac{e_\phi^\infty(T)}{\|\phi(\cdot,T)\|_{H^1}},$$

instead of the absolute errors in (4.2) to compare different numerical methods. Tables 4 and 5 show the temporal errors $\eta_\phi(T=1)$ and $\eta_\psi(T=1)$, respectively, of the MTI-SP method (3.17)–(3.19), while for comparison Table 6 depicts the temporal errors of the EWI-SP method proposed in [5] for the KGZ system (1.3).

From Tables 4–6, we can draw the same conclusions as in §4.1 for the MTI-SP method in term of approximation of ψ in the KGZ system (cf. Table 5); on the contrary, the EWI-SP method doesn't converge uniformly in the approximation of ψ when $0<\varepsilon\ll 1$ (cf. Table 6). Due to that $\psi=O(\varepsilon)$ for $\varepsilon\in(0,1]$, both the MTI-SP and EWI-SP methods converge uniformly and optimally at quadratical convergence rate in the approximation of ϕ (cf. Tables 4 and 6). From this comparison, the

Table 6
Temporal errors of the EWI-SP for the KGZ with (4.11) under $h = 1/8$ for different ε and τ.

$\eta_\phi(T=1)$	$\tau_0 = 0.2$	$\tau_0/2^2$	$\tau_0/2^4$	$\tau_0/2^6$	$\tau_0/2^8$	$\tau_0/2^{10}$
$\varepsilon_0 = 0.5$	2.50E−3	**1.16E−04**	7.15E−6	4.47E−7	2.79E−8	1.81E−9
Rate	–	**2.22**	2.01	2.00	2.00	1.97
$\varepsilon_0/2$	7.00E−3	1.34E−04	**7.69E−6**	4.78E−7	2.99E−8	1.95E−9
Rate	–	2.85	**2.06**	2.00	2.00	1.97
$\varepsilon_0/2^2$	5.65E−4	2.10E−03	3.75E−5	**2.19E−6**	1.37E−7	8.55E−9
Rate	–	–	2.90	**2.05**	2.00	2.00
$\varepsilon_0/2^3$	1.49E−4	1.52E−04	4.98E−4	9.98E−6	**5.83E−7**	3.63E−8
Rate	–	–	–	2.82	**2.05**	2.00
$\varepsilon_0/2^4$	4.01E−5	3.85E−05	3.86E−5	1.41E−4	2.54E−6	**1.48E−7**
Rate	–	–	–	–	2.89	**2.05**
$\varepsilon_0/2^5$	9.87E−6	1.01E−05	9.68E−6	9.69E−6	3.92E−5	6.36E−7
Rate	–	–	–	–	–	2.97
$\varepsilon_0/2^6$	2.46E−6	2.45E−6	2.53E−6	2.42E−6	2.43E−6	1.01E−5
Rate	–	–	–	–	–	–

$\eta_\psi(T=1)$	$\tau_0 = 0.2$	$\tau_0/2^2$	$\tau_0/2^4$	$\tau_0/2^6$	$\tau_0/2^8$	$\tau_0/2^{10}$
$\varepsilon_0 = 0.5$	9.60E−2	**4.70E−3**	2.92E−4	1.96E−5	1.14E−6	6.90E−8
Rate	–	**2.17**	2.01	1.95	2.06	2.02
$\varepsilon_0/2$	1.69E+0	5.31E−2	**3.10E−3**	1.93E−4	1.19E−5	7.28E−7
Rate	–	2.50	**2.05**	2.00	2.01	2.01
$\varepsilon_0/2^2$	7.10E−1	1.98E+0	4.70E−2	**2.70E−3**	1.76E−4	1.05E−5
Rate	–	−0.74	2.70	**2.06**	1.97	2.03
$\varepsilon_0/2^3$	7.39E−1	7.43E−1	3.52E+0	4.57E−2	**2.70E−3**	1.64E−4
Rate	–	0.00	−1.12	3.13	**2.04**	2.02
$\varepsilon_0/2^4$	7.79E−1	7.50E−1	7.52E−1	6.68E+0	4.53E−2	**2.60E−3**
Rate	–	0.03	0.00	−1.58	3.60	**2.06**
$\varepsilon_0/2^5$	7.60E−1	7.87E−1	7.53E−1	7.55E−1	9.85E+0	4.46E−2
Rate	–	−0.03	0.30	0.00	−1.85	3.89
$\varepsilon_0/2^6$	7.70E−1	7.62E−1	7.90E−1	7.53E−1	7.55E−1	1.14E+1
Rate	–	0.01	−0.03	0.03	0.00	−1.96

MTI-SP method performs much better than the EWI-SP method, especially in the high-plasma-frequency limit regime. In fact, under the assumption that $\psi = O(\varepsilon)$, $\partial_t \psi = O(\varepsilon^{-1})$ and $\phi = O(1)$ for $\varepsilon \in (0, 1]$, our numerical results suggest the following error bounds of the MTI-SP method for the KGZ system (1.3) with $\varepsilon \in (0, 1]$

$$\eta_\psi(t_n) \lesssim h^{m_0} + \frac{\tau^2}{\varepsilon^2}, \quad \eta_\psi(t_n) \lesssim h^{m_0} + \tau^2 + \varepsilon^2, \quad \eta_\phi(t_n) \lesssim h^{m_0} + \min\{\varepsilon^2, \tau^2\}, \quad 0 \le n \le \frac{T}{\tau}, \tag{4.12}$$

which immediately imply the following uniform error bound

$$\eta_\psi(t_n) \lesssim h^{m_0} + \min\left\{\frac{\tau^2}{\varepsilon^2}, \tau^2 + \varepsilon^2\right\} \lesssim h^{m_0} + \tau, \quad \eta_\phi(t_n) \lesssim h^{m_0} + \min\{\varepsilon^2, \tau^2\}, \quad 0 \le n \le \frac{T}{\tau},$$

with $m_0 > 0$ depending on the regularity of the solution; and the following error bounds of the EWI-SP method for the KGZ system (1.3) with $\varepsilon \in (0, 1]$

$$\eta_\psi(t_n) \lesssim h^{m_0} + \frac{\tau^2}{\varepsilon^4}, \quad \eta_\phi(t_n) \lesssim h^{m_0} + \min\{\varepsilon^2, \tau^2\}, \quad 0 \le n \le \frac{T}{\tau}. \tag{4.13}$$

Again, rigorous mathematical justification for the above error estimates of the MTI-SP and EWI-SP methods is on-going.

Now we apply the MTI-SP method to study numerically the *orbital stability* of the soliton solution (4.6) of the KGZ system (1.3) in 1D for different $\varepsilon \in (0, 1]$. In order to do so, we take $d = 1$ in (1.3) and choose the initial data in (1.5) as

$$\begin{cases} \psi_0(x) = \psi^s(x, 0; \alpha, k) + \xi\varepsilon(1 + 0.5i)\mathrm{e}^{-(x+1)^2}, \quad \phi_0(x) = \phi^s(x, 0; \alpha, k) + \xi\mathrm{e}^{-(x-1)^2}, \quad x \in \mathbb{R}, \\ \psi_1(x) = \varepsilon^2\partial_t\psi^s(x, 0; \alpha, k) + \xi\varepsilon(1 + 0.5i)\mathrm{e}^{-(x+1)^2}, \quad \phi_1(x) = \partial_t\phi^s(x, 0; \alpha, k) + \xi\mathrm{e}^{-(x-1)^2}, \end{cases} \tag{4.14}$$

where $\xi > 0$ is a parameter to measure the amplitude of the perturbation to the soliton solution at $t = 0$. Again, the KGZ system (1.3) with $d = 1$ and (4.14) is solved numerically on $\Omega = [-16, 16]$ by the MTI-SP method (3.17)–(3.19) with a very fine mesh $h = 1/16$ and a very small time step $\tau = 10^{-5}$. Fig. 4 shows the time evolution of the error

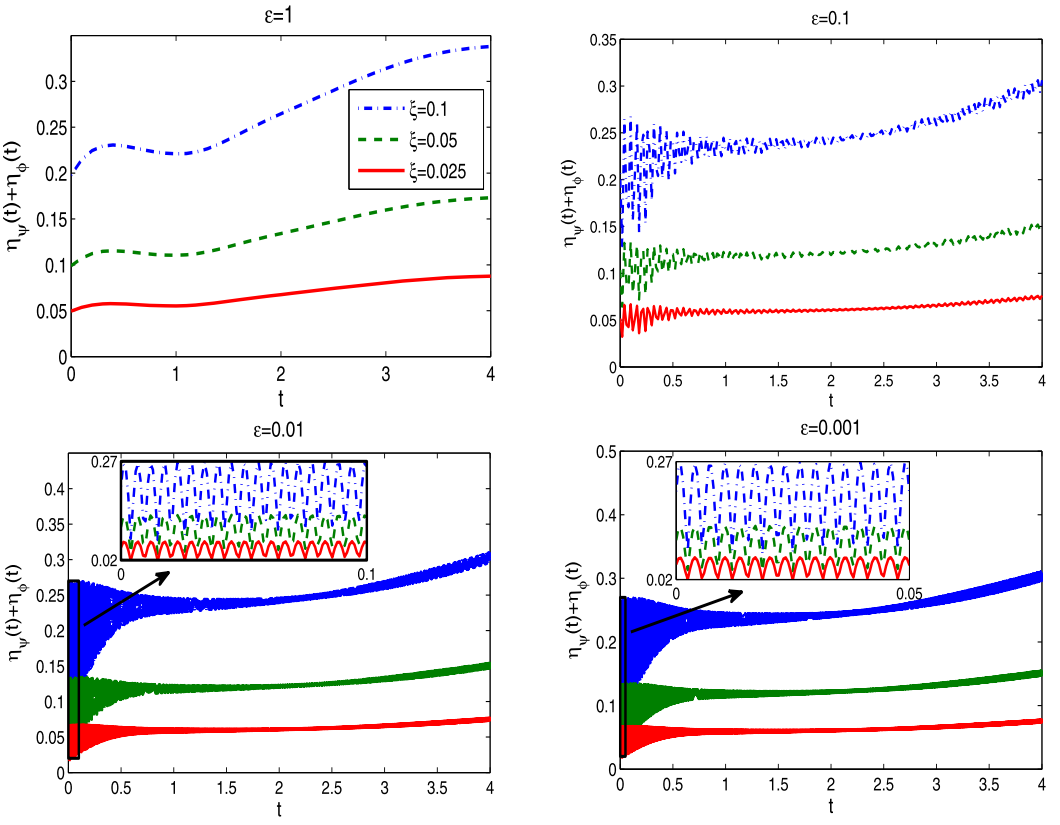

Fig. 4. Time evolution of $\eta_\psi(t)+\eta_\phi(t)$ for the stability of the soliton solution for different ξ and ε.

$$\eta_\psi(t)+\eta_\phi(t)=\frac{\|\psi(\cdot,t)-\psi^s(\cdot,t)\|_{H^2}}{\|\psi^s(\cdot,t)\|_{H^2}}+\frac{\|\phi(\cdot,t)-\phi^s(\cdot,t)\|_{H^1}}{\|\phi^s(\cdot,t)\|_{H^1}},\qquad t\geq 0,$$

for different ξ and ε. From Fig. 4, we can conclude numerically that the soliton solution (4.6) of the KGZ system (1.3) in 1D is dynamically stable for short time and orbitally stable for long time, even in the high-plasma-frequency limit regime.

Next we apply the MTI-SP method to study numerically the *interaction* of the soliton solutions (4.6) of the KGZ system (1.3) in 1D for different $\varepsilon\in(0,1]$. In order to do so, we take $d=1$ in (1.3) and choose the initial data in (1.5) as

$$\begin{cases}\psi_0(x)=\psi^s(x+x_0,0;\alpha_1,k_1)+\psi^s(x-x_0,0;\alpha_2,-k_2),\\ \psi_1(x)=\varepsilon^2\partial_t\psi^s(x+x_0,0;\alpha_1,k_1)+\varepsilon^2\partial_t\psi^s(x-x_0,0;\alpha_2,-k_2),\\ \phi_0(x)=\phi^s(x+x_0,0;\alpha_1,k_1)+\phi^s(x-x_0,0;\alpha_2,-k_2),\qquad x\in\mathbb{R},\\ \phi_1(x)=\partial_t\phi^s(x+x_0,0;\alpha_1,k_1)+\partial_t\phi^s(x-x_0,0;\alpha_2,-k_2),\end{cases}\tag{4.15}$$

where we take $x_0=12$, $k_1=k_2=1$ and $\alpha_j=\delta_j\varepsilon$ satisfying $0<\delta_j\leq\dfrac{\sqrt{2}}{1+\sqrt{2}}:=\delta^{(0)}\approx 0.5858$ for $j=1,2$. Three cases will be considered: Case I. $\delta_1=\delta_2=\dfrac{1}{\sqrt{3}}$; Case II. $\delta_1=\dfrac{1}{\sqrt{10}}$ and $\delta_2=\dfrac{1}{\sqrt{3}}$; and Case III. $\delta_1=\dfrac{1}{\sqrt{2.92}}$ and $\delta_2=\dfrac{1}{\sqrt{3}}$. The problems are solved numerically on $\Omega=[-32,32]$ by the MTI-SP method (3.17)–(3.19) with a very fine mesh $h=1/16$ and a very small time step $\tau=10^{-4}$. Fig. 5 shows the dynamics of $|\psi(x,t)|$ and $\phi(x,t)$ of the collision between two solitons with the same energy, i.e. Case I for different ε; and Fig. 6 depicts similar results for Case II, i.e. with different energy. In addition, Fig. 7 plots the time evolution of $\|\psi(\cdot,t)\|_{L^\infty}$ and $\|\phi(\cdot,t)\|_{L^\infty}$ in Cases I and III for different ε to demonstrate finite time blow-up under certain parameter setups.

From Figs. 5–7, we can draw the following conclusions:

(i) For any fixed $0<\delta_1=\delta_2:=\delta<\delta^{(0)}$ such that $\alpha_1=\alpha_2=\delta\varepsilon$ in (4.15), there exists a critical $\varepsilon_c(\delta)>0$ such that, when $\varepsilon>\varepsilon_c(\delta)$ finite time blow-up happens after the collision of the two solitons, and on the contrary, when $0<\varepsilon<\varepsilon_c(\delta)$ finite

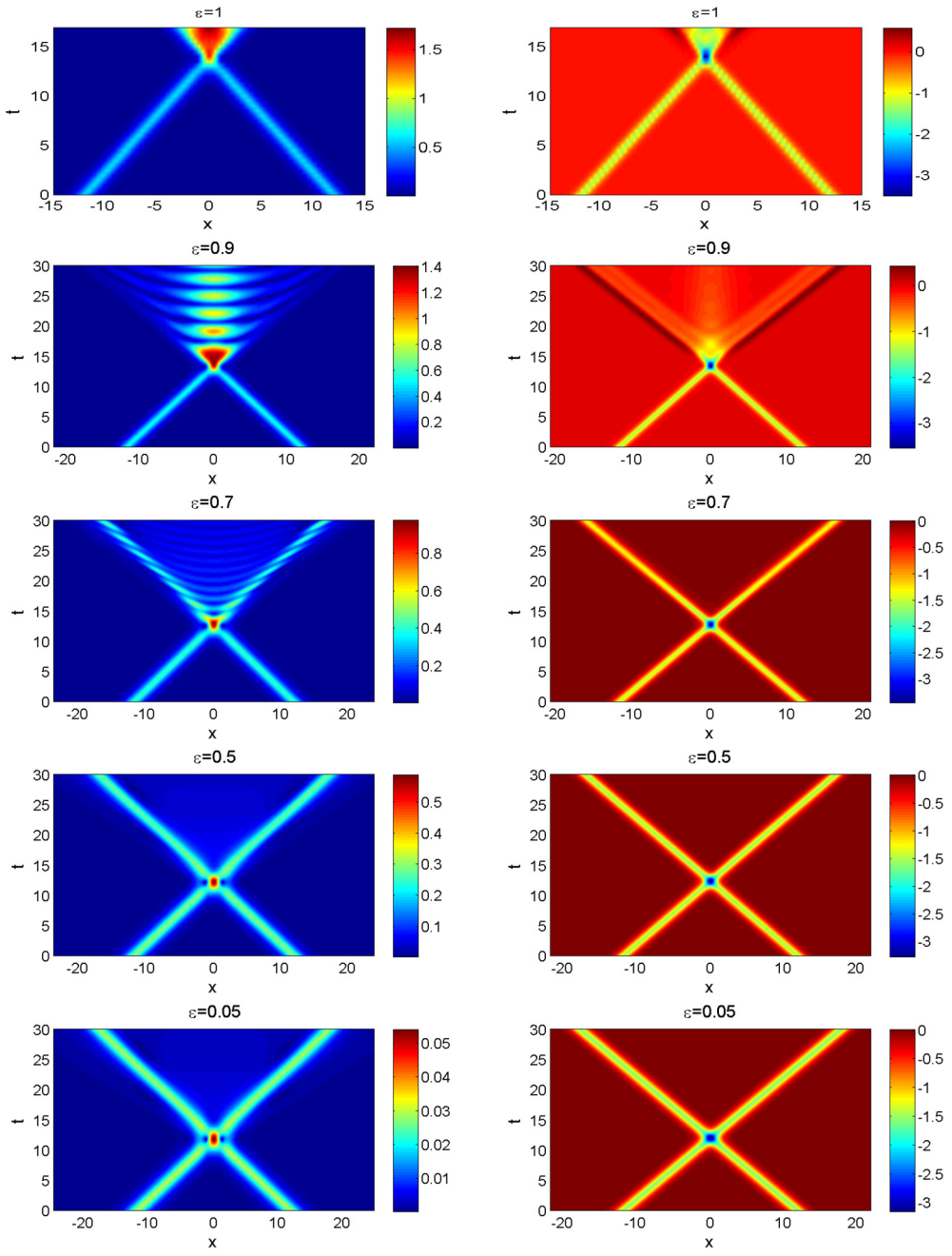

Fig. 5. Contour plots of $|\psi(x,t)|$ (left column) and $\phi(x,t)$ (right column) of the collision between two solitons with the same energy in Case I for different ε.

time blow-up doesn't happen after the collision. Fig. 8 displays the dependence of $\varepsilon_c(\delta)$ vs $0 < \delta \leq \delta^{(0)}$ and the blow-up time $t = T_b$ for different ε and δ. This implies that $\varepsilon_c(\delta)$ almost does not depend on $0 < \delta < \delta^{(0)}$; and for any fixed $\varepsilon > \varepsilon_c(\delta)$, the blow-up time T_b decreases when δ increases; for any fixed $0 < \delta < \delta^{(0)}$, the blow-up time T_b decreases when $\varepsilon > \varepsilon_c(\delta)$ increases. Based on our additional numerical results not shown here for brevity, we also find that when $|\delta_1 - \delta_2|$ is large enough, there exists no finite time blow-up for $\varepsilon \in (0, 1]$ (cf. Fig. 6).

(ii) After the collision of the two solitons, sound and other waves are generated, which demonstrate that the KGZ system (1.3) in 1D is not an integrable system. In addition, for fixed $0 < \delta_1 < \delta^{(0)}$ and $0 < \delta_2 < \delta^{(0)}$, when $0 < \varepsilon \leq 1$ is small enough; or for fixed $\varepsilon \in (0, 1]$, when $|\delta_1 - \delta_2|$ is large enough, the collision of the two solitons is quite elastic (cf. Figs. 5 (bottom two rows) and 6).

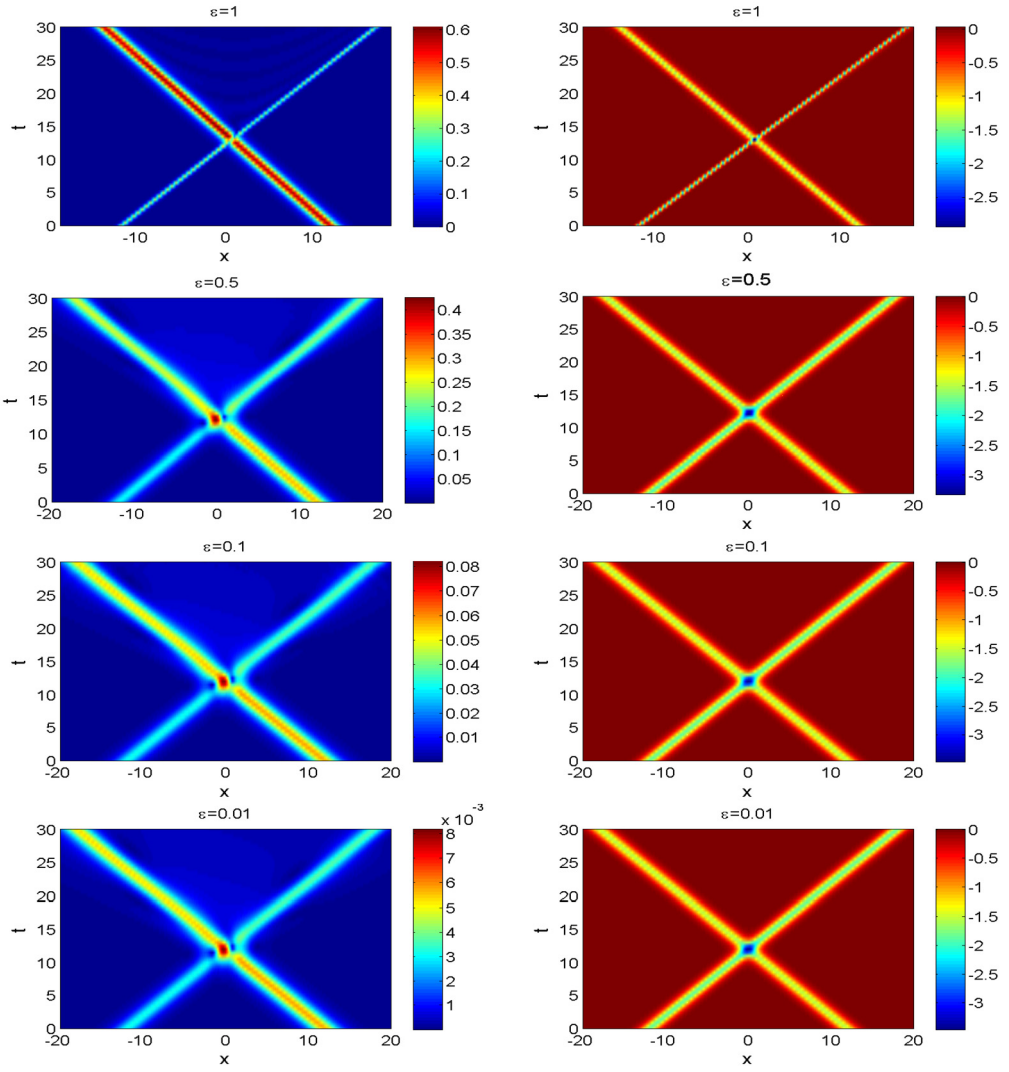

Fig. 6. Contour plots of $|\psi(x,t)|$ (left column) and $\phi(x,t)$ (right column) of the collision between two solitons with different energy in Case II for different ε.

4.4. Application to wave interactions in 2D

In order to do so, we take $d=2$ in (1.3) and choose the initial data in (1.5) as

$$\begin{cases} \psi_0(x,y)=\exp\left(-(x+2)^2-y^2\right)+\exp\left(-(x-2)^2-y^2\right), \quad \psi_1(x,y)=\exp\left(-x^2-y^2\right), \\ \phi_0(x,y)=\operatorname{sech}(x^2+(y+2)^2)+\operatorname{sech}(x^2+(y-2)^2), \quad \phi_1(x,y)=\operatorname{sech}(x^2+y^2), \quad (x,y)\in\mathbb{R}^2. \end{cases} \tag{4.16}$$

The problem is solved numerically on $\Omega=[-32,32]^2$ by the MTI-SP method (3.17)–(3.19) with a very fine mesh $h=1/16$ and a very small time step $\tau=10^{-4}$. Fig. 9 shows contour plots of the solution for different t and $0<\varepsilon\leq 1$. From this result, we can see that the MTI-SP method can be used to efficiently and accurately simulate wave dynamics and interaction of the KGZ system (1.3) in high dimensions.

5. Conclusions

A multiscale time integrator sine pseudospectral (MTI-SP) method was proposed for solving the Klein–Gordon–Zakharov (KGZ) system with a dimensionless parameter $0<\varepsilon\leq 1$ which is inversely proportional to the plasma frequency. The solution of the KGZ system is highly oscillatory in time in the high-plasma-frequency limit regime, i.e. $0<\varepsilon\ll 1$. The key ideas for designing the MTI-SP method were based on (i) carrying out a multiscale decomposition by frequency at each time step with proper choice of transmission conditions between time steps, and (ii) adapting the sine spectral method

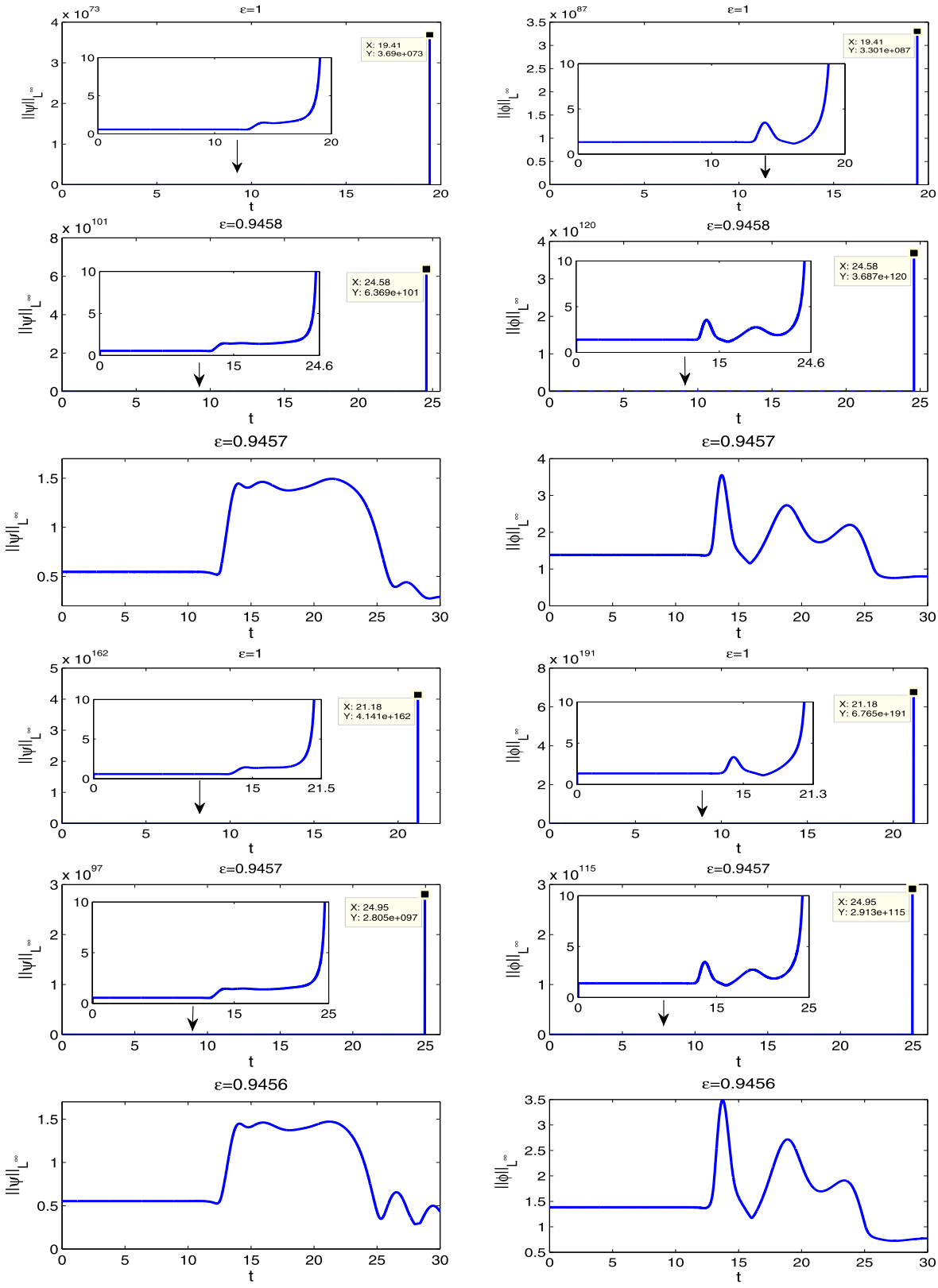

Fig. 7. Time evolution of $\|\psi(\cdot,t)\|_{L^\infty}$ (left column) and $\|\phi(\cdot,t)\|_{L^\infty}$ (right column) of the collision between two solitons in Case I (top three rows) and Case III (bottom three rows) for different ε.

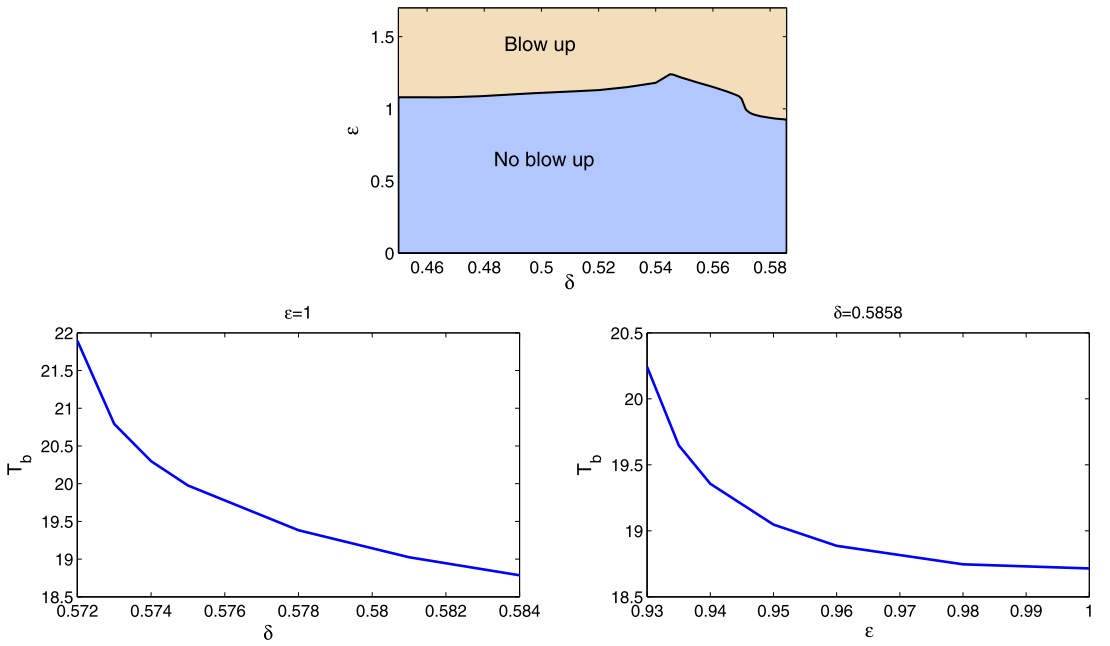

Fig. 8. The phase diagram (top row) on finite time blow-up after collisions between two solitons with the same energy in \$4.3 for different ε and δ; and the blow-up time T_b vs δ for $\varepsilon = 1$ (bottom left) and vs ε for $\delta = 0.5858$ (bottom right).

for spatial discretization and the exponential wave integrators (EWIs) for integrating second-order highly oscillating ODEs in phase space. Extensive numerical results demonstrated that the MTI-SP method converges uniformly and optimally in space with spectral convergence rate if the solution is smooth, and uniformly in time with linear convergence rate for $\varepsilon \in (0, 1]$ and optimally with quadratic convergence rate in the regimes when either $\varepsilon = O(1)$ or $0 < \varepsilon \leq \tau$. Comparisons with the existing EWI-SP method proposed in [5] were carried out to show the advantage of the MTI-SP method, especially in the high-plasma-frequency limit regime. Finally, we applied the MTI-SP to study convergence rates of the solution of the KGZ system to those of its limiting models in the high-plasma-frequency limit regime, stability and interactions of soliton solutions of the KGZ system in 1D with different parameter regimes, and wave dynamics and interaction of the KGZ system in 2D. Our numerical results identified explicitly certain initial data and parameter regimes such that the KGZ system in 1D will blow up at finite time.

Acknowledgements

This work was supported by the Academic Research Fund of Ministry of Education of Singapore grant No. R-146-000-223-112. Part of the work was done when the authors were visiting the Institute for Mathematical Sciences at the National University of Singapore in 2015.

Appendix A. Explicit formulas for the coefficients used in (3.16) for the MTI-SP method

For the coefficients in (3.16) used in the MTI-SP method, after a detailed computation, we have

$$c_l = \frac{\lambda_l^- e^{i\tau\lambda_l^+} - \lambda_l^+ e^{i\tau\lambda_l^-} + \lambda_l^+ - \lambda_l^-}{\varepsilon^2(\lambda_l^- - \lambda_l^+)\lambda_l^+\lambda_l^-}, \qquad p_l = \frac{\varepsilon^2\mu_l\left[\varepsilon^2\mu_l e^{\frac{2i\tau}{\varepsilon}} - \varepsilon^2\mu_l\cos(\mu_l\tau) - 2i\sin(\mu_l\tau)\right]}{\varepsilon^4\mu_l^2 - 4},$$

$$q_l = \frac{\varepsilon^4\mu_l\left[4i\varepsilon^2\mu_l\cos(\mu_l\tau) + \mu_l e^{\frac{2i\tau}{\varepsilon}}(\tau\varepsilon^4\mu_l^2 - 4\tau - 4i\varepsilon^2) - (4+\varepsilon^2\mu_l^2)\sin(\mu_l\tau)\right]}{(\varepsilon^4\mu_l^2 - 4)^2},$$

$$d_l = i\frac{(\lambda_l^-)^2 e^{i\tau\lambda_l^+} - (\lambda_l^+)^2 e^{i\tau\lambda_l^-} + i\tau\lambda_l^+\lambda_l^-(\lambda_l^+ - \lambda_l^-) + (\lambda_l^+)^2 - (\lambda_l^-)^2}{\varepsilon^2(\lambda_l^+ - \lambda_l^-)(\lambda_l^+\lambda_l^-)^2}, \quad 1 \leq l \leq N-1,$$

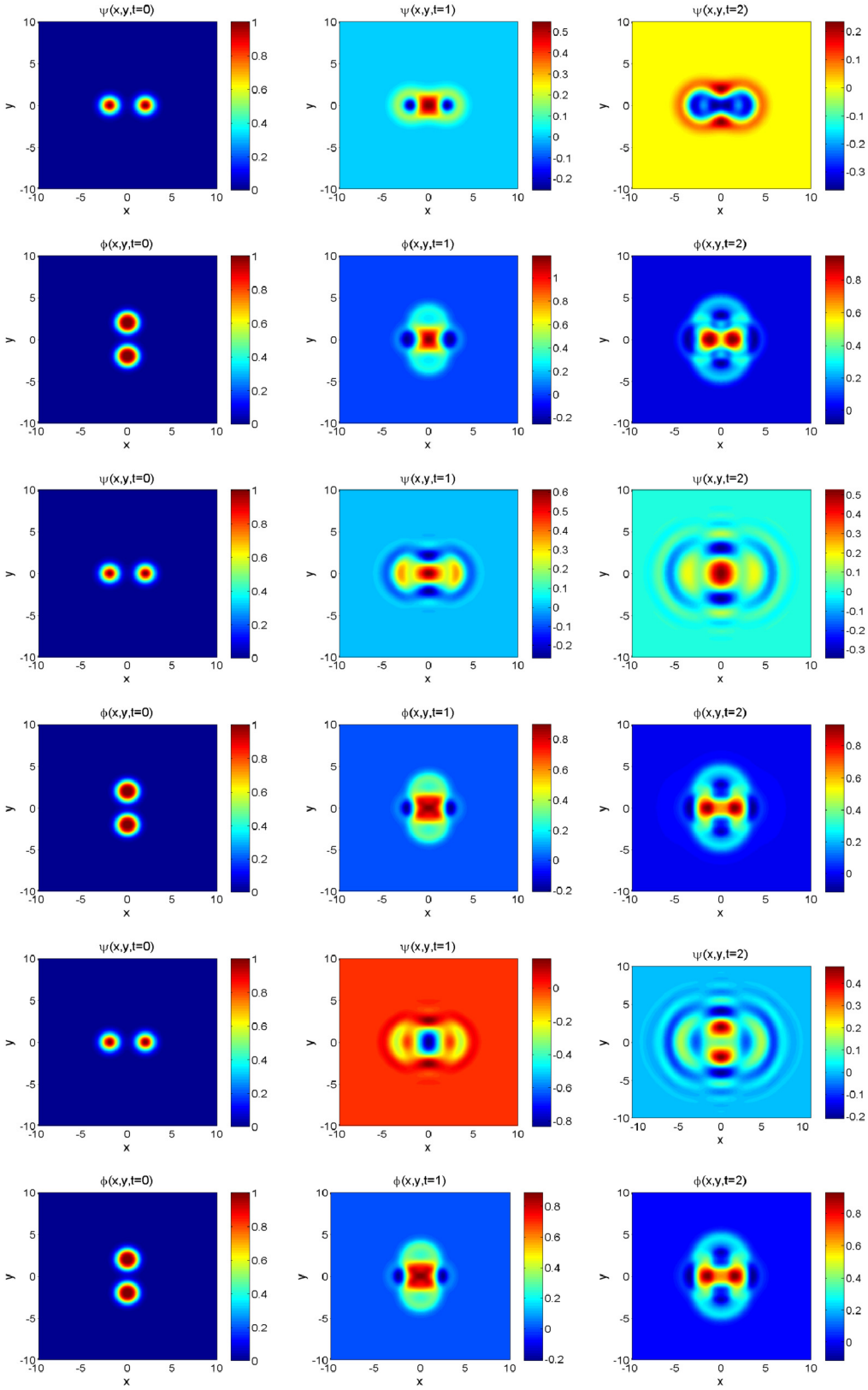

Fig. 9. Contour plots of the solution of the KGZ (1.3) in 2D with (4.16) at different t for $\varepsilon = 1$ (first two rows), $\varepsilon = 0.1$ (second two rows) and $\varepsilon = 0.01$ (last two rows).

$$\dot{c}_l = i\frac{e^{i\tau\lambda_l^+} - e^{i\tau\lambda_l^-}}{\varepsilon^2(\lambda_l^- - \lambda_l^+)}, \qquad \dot{d}_l = c_l, \qquad \dot{p}_l = \frac{\varepsilon^2\mu_l^2\left[2ie^{\frac{2i\tau}{\varepsilon}} - 2i\cos(\mu_l\tau) + \varepsilon^2\mu_l\sin(\mu_l\tau)\right]}{\varepsilon^4\mu_l^2 - 4},$$

$$\dot{q}_l = \frac{\mu_l^4\left[\varepsilon^2 e^{\frac{2i\tau}{\varepsilon}}(4\varepsilon^4 - 8i\tau + \varepsilon^6\mu_l^2 + 2i\tau\varepsilon^4\mu_l^2) - \varepsilon^4(4 + \varepsilon^4\mu_l^2)\cos(\mu_l\tau) - 4i\varepsilon^6\mu_l\sin(\mu_l\tau)\right]}{(\varepsilon^4\mu_l^2 - 4)^2}.$$

References

[1] W. Bao, Y. Cai, Uniform error estimates of finite difference methods for the nonlinear Schrödinger equation with wave operator, SIAM J. Numer. Anal. 50 (2012) 492–521.
[2] W. Bao, Y. Cai, Uniform and optimal error estimates of an exponential wave integrator sine pseudospectral method for the nonlinear Schrödinger equation with wave operator, SIAM J. Numer. Anal. 52 (2014) 1103–1127.
[3] W. Bao, Y. Cai, X. Zhao, A uniformly accurate multiscale time integrator pseudospectral method for the Klein–Gordon equation in the nonrelativistic limit regime, SIAM J. Numer. Anal. 52 (2014) 2488–2511.
[4] W. Bao, X. Dong, Analysis and comparison of numerical methods for the Klein–Gordon equation in the nonrelativistic limit regime, Numer. Math. 120 (2012) 189–229.
[5] W. Bao, X. Dong, X. Zhao, An exponential wave integrator sine pseudospectral method for the Klein–Gordon–Zakharov system, SIAM J. Sci. Comput. 25 (2013) A2903–A2927.
[6] W. Bao, X. Dong, X. Zhao, Uniformly accurate multiscale time integrators for highly oscillatory second order differential equations, J. Math. Study 47 (2014) 111–150.
[7] W. Bao, F. Sun, Efficient and stable numerical methods for the generalized and vector Zakharov system, SIAM J. Sci. Comput. 26 (2005) 1057–1088.
[8] W. Bao, F. Sun, G.W. Wei, Numerical methods for the generalized Zakharov system, J. Comput. Phys. 190 (2003) 201–228.
[9] W. Bao, X. Zhao, A uniformly accurate (UA) multiscale time integrator Fourier pseudospectral method for the Klein–Gordon-Schrödinger equations in the nonrelativistic limit regime, Numer. Math. (2016), http://dx.doi.org/10.1007/s00211-016-0818-x.
[10] L. Bergé, B. Bidégaray, T. Colin, A perturbative analysis of the time-envelope approximation in strong Langmuir turbulence, Physica D 95 (1996) 351–379.
[11] P.M. Bellan, Fundamentals of Plasmas Physics, Cambridge University Press, Cambridge, 2006.
[12] Ph. Chartier, N. Crouseilles, M. Lemou, F. Méhats, Uniformly accurate numerical schemes for highly oscillatory Klein–Gordon and nonlinear Schrödinger equations, Numer. Math. 129 (2015) 211–250.
[13] D. Cohen, E. Hairer, Ch. Lubich, Modulated Fourier expansions of highly oscillatory differential equations, Found. Comput. Math. 3 (2003) 327–345.
[14] R.-O. Dendy, Plasma Dynamics, Oxford University Press, Oxford, 1990.
[15] P. Deuflhard, A study of extrapolation methods based on multistep schemes without parasitic solutions, Z. Angew. Math. Phys. 30 (1979) 177–189.
[16] E. Faou, K. Schratz, Asymptotic preserving schemes for the Klein–Gordon equation in the nonrelativistic limit regime, Numer. Math. 126 (2014) 441–469.
[17] W. Gautschi, Numerical integration of ordinary differential equations based on trigonometric polynomials, Numer. Math. 3 (1961) 381–397.
[18] D. Gottlieb, S.A. Orszag, Numerical Analysis of Spectral Methods: Theory and Applications, Society for Industrial and Applied Mathematics, Philadelphia, 1993.
[19] V. Grimm, A note on the Gautschi-type method for oscillatory second-order differential equations, Numer. Math. 102 (2005) 61–66.
[20] V. Grimm, On error bounds for the Gautschi-type exponential integrator applied to oscillatory second-order differential equations, Numer. Math. 100 (2005) 71–89.
[21] J.S. Hesthaven, S. Gottlieb, D. Gottlieb, Spectral Methods for Time-Dependent Problems, Cambridge University Press, Cambridge, New York, 2007.
[22] M. Hochbruck, Ch. Lubich, A Gautschi-type method for oscillatory second-order differential equations, Numer. Math. 83 (1999) 402–426.
[23] E. Hairer, Ch. Lubich, G. Wanner, Geometric Numerical Integration, Springer-Verlag, 2002.
[24] M.S. Ismail, A. Biswas, 1-soliton solution of the Klein–Gordon–Zakharov equation with power law nonlinearity, Appl. Math. Comput. 217 (2010) 4186–4196.
[25] S. Klainerman, M. Machedon, Space–time estimates for null forms and the local existence theorem, Commun. Pure Appl. Math. 46 (1993) 1221–1268.
[26] N. Masmoudi, K. Nakanishi, From the Klein–Gordon–Zakharov system to the nonlinear Schrödinger equation, J. Hyperbolic Differ. Equ. 2 (2005) 975–1008.
[27] N. Masmoudi, K. Nakanishi, Energy convergence for singular limits of Zakharov type systems, Invent. Math. 172 (2008) 535–583.
[28] N. Masmoudi, K. Nakanishi, From nonlinear Klein–Gordon equation to a system of coupled nonlinear Schrödinger equations, Math. Ann. 324 (2002) 359–389.
[29] D.R. Nicholson, Topics in strong Langmuir turbulence, Phys. Scr. 27 (1983) 77–82.
[30] T. Ozawa, K. Tsutaya, Y. Tsutsumi, Well-posedness in energy space for the Cauchy problem of the Klein–Gordon–Zakharov equations with different propagation speeds in three space dimensions, Math. Ann. 313 (1999) 127–140.
[31] J. Shen, T. Tang, L. Wang, Spectral Methods: Algorithms, Analysis and Applications, Springer, 2011.
[32] J.M. Sanz-Serna, Modulated Fourier expansions and heterogeneous multiscale methods, IMA J. Numer. Anal. 29 (2009) 595–605.
[33] B. Texier, Derivation of the Zakharov equations, Arch. Ration. Mech. Anal. 184 (2007) 121–183.
[34] H. Triki, N. Boucerredj, Soliton solutions of the Klein–Gordon–Zakharov equations with power law nonlinearity, Appl. Math. Comput. 227 (2014) 341–346.
[35] J. Wang, Solitary wave propagation and interactions for the Klein–Gordon–Zakharov equations in plasma physics, J. Phys. A, Math. Theor. 42 (2009) 085205.
[36] T. Wang, J. Chen, L. Zhang, Conservative difference methods for the Klein–Gordon–Zakharov equations, J. Comput. Appl. Math. 205 (2007) 430–452.
[37] V. Zakharov, Collapse of Langmuir waves, Sov. Phys. JETP 35 (1972) 908–914.
[38] X. Zhao, On error estimates of an exponential wave integrator sine pseudospectral method for the Klein–Gordon–Zakharov system, Numer. Methods Partial Differ. Equ. 32 (2016) 266–291.